Journal of Autoimmunity 86 (2018) 75–92

Contents lists available at ScienceDirect

Journal of Autoimmunity

journal homepage: www.elsevier.com/locate/jautimm

Paradoxical development of polymyositis-like autoimmunity through augmented expression of autoimmune regulator (AIRE)

Hitoshi Nishijima [a], Tatsuya Kajimoto [a], Yoshiki Matsuoka [a], Yasuhiro Mouri [a], Junko Morimoto [a], Minoru Matsumoto [a, b], Hiroshi Kawano [a, c], Yasuhiko Nishioka [c], Hisanori Uehara [b], Keisuke Izumi [b], Koichi Tsuneyama [b], Il-mi Okazaki [d], Taku Okazaki [d], Kazuyoshi Hosomichi [e], Ayako Shiraki [f], Makoto Shibutani [f], Kunitoshi Mitsumori [f], Mitsuru Matsumoto [a, g, *]

[a] Division of Molecular Immunology, Institute for Enzyme Research, Tokushima University, Tokushima 770-8503, Japan
[b] Department of Molecular and Environmental Pathology, Institute of Biomedical Sciences, The University of Tokushima Graduate School, Tokushima 770-8503, Japan
[c] Department of Respiratory Medicine and Rheumatology, Institute of Biomedical Sciences, The University of Tokushima Graduate School, Tokushima 770-8503, Japan
[d] Division of Immune Regulation, Institute for Genome Research, Tokushima University, Tokushima 770-8503, Japan
[e] Department of Bioinformatics and Genomics, Graduate School of Medical Sciences, Kanazawa University, Ishikawa 920-0934, Japan
[f] Laboratory of Veterinary Pathology, Tokyo University of Agriculture and Technology, Tokyo 183-8509, Japan
[g] AMED-CREST, Japan Agency for Medical Research and Development, Tokyo 100-0004, Japan

ARTICLE INFO

Article history:
Received 12 July 2017
Received in revised form
13 September 2017
Accepted 13 September 2017
Available online 18 September 2017

Keywords:
Medullary thymic epithelial cell (mTEC)
AIRE
Muscle
Tolerance

ABSTRACT

Autoimmunity is prevented by the function of the autoimmune regulator [*AIRE* (*Aire* in mice)], which promotes the expression of a wide variety of tissue-restricted antigens (TRAs) from medullary thymic epithelial cells (mTECs) and from a subset of peripheral antigen-presenting cells (APCs). We examined the effect of additive expression of human AIRE (huAIRE) in a model of autoimmune diabetes in NOD mice. Unexpectedly, we observed that mice expressing augmented AIRE/Aire developed muscle-specific autoimmunity associated with incomplete maturation of mTECs together with impaired expression of Aire-dependent TRAs. This led to failure of deletion of autoreactive T cells together with dramatically reduced production of regulatory T cells in the thymus. In peripheral APCs, expression of costimulatory molecules was augmented. We suggest that levels of Aire expression need to be tightly controlled for maintenance of immunological tolerance. Our results also highlight the importance of coordinated action between central tolerance and peripheral tolerance under the common control of Aire.

1. Introduction

Development of harmful autoimmunity is prevented by two distinct but functionally cooperative mechanisms: central tolerance established in the thymus and peripheral tolerance operational outside the thymus. In the thymus, autoreactive T cells are eliminated by clonal deletion through interaction with self-antigens presented by medullary thymic epithelial cells (mTECs) and/or dendritic cells (DCs) that reside in the thymus [1]. The thymus also contains a population of B cells that preferentially co-localize with DCs and mTECs, and their role in central tolerance has also been suggested [2,3]. This process of negative selection, however, does not seem to be perfect, and some T cells are capable of reacting with

Abbreviations: Ab, antibody; APC, antigen-presenting cell; BM, bone marrow; Crp, C-reactive protein; cTEC, cortical thymic epithelial cell; DC, dendritic cell; EpCAM, epithelial cell adhesion molecule 1; eTAC, extrathymic Aire-expressing cell; FISH, fluorescence in situ hybridization; huAIRE, human AIRE; Ins2, insulin 2; mAb, monoclonal Ab; MHC-II, MHC class II; mTEC, medullary thymic epithelial cell; Myh7, myosin heavy chain 7; OVA, ovalbumin; RIP, rat insulin promoter; Sap, salivary protein 1; Tg, transgenic mice; TRA, tissue-restricted antigen; Treg, regulatory T cell; UEA-1, *Ulex europaeus* agglutinin 1.

* Corresponding author. Division of Molecular Immunology, Institute for Enzyme Research, Tokushima University, 3-18-15 Kuramoto, Tokushima 770-8503, Japan.
E-mail address: mitsuru@tokushima-u.ac.jp (M. Matsumoto).

http://dx.doi.org/10.1016/j.jaut.2017.09.006

self-antigens in the periphery [4,5]. It has been suggested that the major function of regulatory T cells (Tregs) is to maintain these autoreactive T cells in an anergic state [6]. Thus, cooperation between central tolerance and peripheral tolerance is essential for prevention of autoimmunity.

One of the best characterized factors within mTECs that contribute to the expression of tissue-restricted antigens (TRAs), thereby contributing to central tolerance, is the autoimmune regulator [*AIRE* (*Aire* in mice)]: mutations in *AIRE* cause autoimmune polyendocrine syndrome type 1 (OMIM 240300) [7]. Loss of Aire in mice has been demonstrated to result in defective expression of many TRAs, consequently allowing the escape of autoreactive T cells [8–10] and impaired Treg production [11,12]. As well as mTECs, Aire expression has been demonstrated in bone marrow (BM)-derived non-conventional antigen-presenting cells (APCs) that show major histocompatibility complex (MHC) class II (MHC-II)^{high} expression as a distinct tolerogenic cell population in secondary lymphoid organs, so-called extrathymic Aire-expressing cells (eTACs) [13,14]. Thus, Aire exerts its tolerogenic function not only within the thymic microenvironment but also in the periphery [15].

Based on these findings, we examined the effect of augmented Aire expression in NOD mice, in which insulin is a primary autoantigen for the development of type I diabetes [16]. Of note, *insulin 2* (*Ins2*) is a prototypic TRA in mTECs whose expression level is strongly affected by loss of Aire [10]. Because of the action of Aire for activation of TRA expression in both mature MHC-II^{high} mTECs and a subset of peripheral APCs exhibiting MHC-II^{high} [14], we achieved augmented Aire expression in NOD mice with the use of the MHC-II promoter, resulting in an unexpected outcome: mice expressing augmented AIRE/Aire developed muscle-specific autoimmunity associated with incomplete maturation of mTECs and impaired expression of Aire-dependent TRAs.

2. Materials and methods

2.1. Mice

Mice expressing huAIRE under control of the MHC-II promoter (pDOI-5) [17] were generated by pronuclear injection of DNA into NOD mouse eggs. In brief, a 1.6-kb cDNA fragment encoding the entire huAIRE protein was ligated into the *Eco*RI site in exon 3 of the rabbit β-globin gene, resulting in the generation of a linearized 5.5-kb *Xba*I-*Nru*I fragment for the injection. Aire-deficient mice on a NOD background have been reported previously [18]. NOD/ShiJic-*scid* Jcl mice and Rag2-deficient mice on a C57BL/6 background were obtained from CLEA Japan Inc. and Taconic, respectively. Rag2-deficient mice were backcrossed onto NOD for more than four generations in our laboratory. B-cell-deficient NOD mice [19,20] and OT-II Tg mice [21] were purchased from the Jackson Laboratory. Tg mice expressing OVA under control of the rat insulin promoter (RIP-OVA Tg) [22] were kindly provided by Dr. MJ. Bevan (Department of Immunology, Howard Hughes Medical Institute, University of Washington, Seattle, WA). The mice were maintained under pathogen-free conditions, and handled in accordance with the Guidelines for Animal Experimentation of Tokushima University School of Medicine.

2.2. Immunohistochemistry

Tissues were harvested, embedded in OCT compound (Sakura Finetek), and frozen at −80 °C. Frozen tissue sections were fixed in acetone. Immunohistochemical analysis of the thymus using rabbit polyclonal anti-huAIRE antibody (Ab) (prepared in our laboratory), rat anti-huAIRE mAb (eBioscience), rat anti-mouse Aire mAb (clone RF33-1 prepared in our laboratory) and anti-epithelial cell adhesion molecule 1 (EpCAM) mAb (eBioscience) was performed as described previously [23,24]. Anti-CD4, anti-CD11b and F4/80 monoclonal Abs (mAbs) were from BioLegend.

2.3. Pathology

Formalin-fixed tissue sections were subjected to H&E staining, and two pathologists independently evaluated the histology without being informed of the detailed condition of each individual mouse.

2.4. TEC preparation and flow-cytometric analysis

Preparation of TECs and flow-cytometric analysis with a FACSCalibur (BD) and a FACSAria II (BD) were performed as described previously [25]. In brief, thymic lobes were isolated from mice and cut into small pieces. The fragments were pipetted to remove the majority of thymocytes in RPMI 1640 medium (Gibco) supplemented with 10% heat-inactivated FCS (Bovogen), 20 mM HEPES, 50 U/ml penicillin, 50 μg/ml streptomycin, and 50 μM 2-ME, hereafter referred to as R10. The resulting thymic fragments were digested with 0.15% collagenase D (Roche) and 10 U/ml DNase I (Roche) in R10 at 37 °C for 30 min. The supernatants, containing dissociated TECs, were saved, and the remaining thymic fragments were digested with 0.15% collagenase/dispase (Roche) and DNase I at 37 °C for 30 min. The supernatants from this digest were combined with the supernatants from the collagenase digests, and the mixture was centrifuged for 5 min at 400 × *g*. The cells were suspended in PBS containing 5 mM EDTA and 1% BSA, and kept on ice until the staining. The mAbs used were anti-CD45, anti-Ly51, anti-CD80, anti-CD86, anti-PD-L1, anti-PD-L2, anti-CD40, anti-CD8α, B220, anti-CD19, anti-Foxp3 and anti-I-A/I-E, all purchased from eBioscience. Anti-CD3ε, anti-CD4 and anti-EpCAM mAbs were from BioLegend. Anti-I-A^{d}, anti-TCR/Vα2 and anti-TCR/Vβ5 were from BD Biosciences. *Ulex europaeus* agglutinin 1 (UEA-1) was from Vector Laboratories.

2.5. Bone marrow (BM) transfer

BM transfer was performed as described previously [26]. In brief, BM cells were suspended in R10 medium containing anti-CD90 (Thy1.2) mAb (clone 30-H12; BioLegend) plus low-toxicity rabbit complement (Cedarlane Laboratories). After incubation at 37 °C for 45 min, the cells were washed twice and adjusted to 5 × 10^{7} viable cells/ml in R10 not containing FCS. Each recipient mouse was then lethally irradiated (9 Gy) and treated with 0.2 ml of donor BM cells *i.v.* on the same day.

2.6. Transfer of T cells into NOD.scid mice

T cells were isolated from the spleen, as described previously [18]. In brief, the spleen cell suspensions were depleted of red blood cells by osmotic lysis, and T cells were purified using biotinylated mAb cocktails containing anti-B220, anti-CD11b, anti-CD11c, anti-CD49b and TER-119 with streptavidin MicroBeads (Miltenyi Biotec). The resulting preparations contained approximately 90% CD3ε^{+} cells. The purified T cells were injected *i.v.* (5 x 10^{6} cells per mouse), and development of the disease and/or diabetes was monitored.

2.7. Suppressive activity of Tregs assessed in vivo and in vitro

CD25^{+} Tregs were isolated from the spleen of wild-type NOD or homozygous huAIRE-Tg at the age of 6–8 weeks. Two million cells

were *i.v.* injected into untreated homozygous huAIRE-Tg at the age of 3–5 weeks old, and their survival was monitored. For *in vitro* suppression assay, $CD4^+$ T cells isolated from the wild-type NOD spleen were labeled with 5-(and-6)-carboxyfluorescein diacetate succinimidyl ester (CFSE). They were then mixed with $CD4^+CD25^+$ Tregs isolated using a Regulatory T Cell Isolation Kit (Miltenyi Biotec) at a 2:1 ratio in the presence of CD3/CD28 Ab beads (Thermo Fisher). Cell division was assessed 72 h after mixing the cells.

2.8. Real-time PCR

RNA was extracted from TECs using RNeasy Mini Kits (QIAGEN) and converted to cDNA with SuperScript III or VILO RT Kits (Invitrogen) in accordance with the manufacturer's instructions. Real-time PCR for quantification of the *insulin 2* (*Ins2*), *salivary protein 1* (*SAP1*), *C-reactive protein* (*CRP*), *myosin heavy chain 7* (*Myh7*), *mouse Aire* (*Aire*), *human AIRE* (*huAIRE*), *ovalbumin* (*OVA*) and *Hprt* genes was performed as described previously [18,23,25]. Detailed sequence information is provided in Supplemental Table 1.

2.9. Fluorescence in situ hybridization (FISH)

Splenocytes isolated from huAIRE-Tg line 1m4L were stimulated with PHA-M (3 μg/ml, Sigma-Aldrich), concanavalin A (3 μg/ml, Sigma-Aldrich) and lipopolysaccharide (10 μg/m, Sigma-Aldrich) for 2 days, followed by addition of demecolcine (0.02 μg/ml: Sigma-Aldrich) for 2 h. The cells were then suspended in 0.075 M KCl for 15 min. FISH analysis was performed using fixed metaphase spreads of splenocytes on slides using biotin-labeled huAIRE cDNA (1.6-kb *Eco*RI/*Sal*I fragment). After hybridization at 37 °C overnight, the slides were incubated with Alexa Fluor 488 streptavidin (Life Technologies) at 37 °C for one hour. One round of amplification with biotinylated anti-avidin (Vector) and a second detection with Alexa Fluor 488 streptavidin were performed to visualize the signal (Takiguchi et al., 2014; Tomizuka et al., 1997). After washing the slides, chromosomal DNA was counterstained with DAPI (Sigma-Aldrich), and images were captured using a Zeiss Axio Imager 2 (Zeiss).

2.10. RNA-seq analysis

Total RNAs from sorted $mTEC^{high}$ were isolated using an RNeasy Mini Kit (Qiagen) following the manufacturers' instructions. Eluted RNAs were incubated with RT-grade DNase (Nippon Gene) for 10 min at room temperature, followed by purification on an RNeasy column (Qiagen). RNAs were verified quantitatively and qualitatively using an Agilent RNA 6000 Pico Kit run on an Agilent 2100 Bioanalyzer (Agilent Technologies). RNA Integrity Numbers were more than 7. Three independent biological replicates from each genotype were used for RNA-seq analysis. Sequencing libraries were generated from 1.0 ng of total RNA with Ovation SoLo RNA-Seq Systems (NuGEN). The libraries were size-selected with AMPure XP beads (Agilent Technologies) and used for cluster generation on the flow cells. Single-end 150-bp sequencing was performed with Illumina MiSeq (Illumina), which generated 5.8–20 x 10^6 sequenced fragments per sample. Prior to alignment, the reads were trimmed to remove adapter sequences. Reads were mapped to the mouse reference genome GRCm38/mm10 using the STAR aligner with option: -outSAMtype BAM SortedByCoordinate to generate a sorted BAM format. Differential gene expression between the experimental samples was analyzed with Cufflinks. Read count tables and group comparisons for differential expression analysis were performed with Cuffdiff, a part of the Cufflinks package. The false-discovery rate (FDR) for detection of differentially abundant transcripts was set to 5%. The data set associated with this project has been submitted to DDBJ Sequence Reads Archive (DRA accession number: DRA005738 and DRA005834).

2.11. Microarray analysis

Splenic B cells ($Thy1^-CD11c^-B220^+$ cells) were isolated from two heterozygous 2m9L huARE-Tg and two non-Tg littermates at 8 weeks of age using a MACS column (Miltenyi Biotec). No technical replicates were used. Total RNA from B cells was isolated using a High Pure RNA Isolation Kit (Roche), and purity of the RNA was assessed using an Agilent 2100 Bioanalyzer. cDNA synthesis was performed using a SuperScript II Reverse Transcriptase (Thermo Fisher). cDNA was fragmented and end-labeled with the Encore Biotin Module (TaKaRa) in accordance with the manufacturer's instructions. Approximately 5 μg of labeled DNA target was hybridized to the Affymetrix Mouse Genome 430 2.0 Array. Data were analyzed using the GeneSpring GX13.0 software package (Agilent Technologies) and deposited to Gene Expression Omnibus (GEO) under the accession number GSE99368.

2.12. Immunoblot analysis

Myosin was purified from heart and soleus muscle of wild-type NOD mice as described previously [27]. Briefly, tissues were homogenized and washed five times with 30 mM KCl, 10 mM phosphate (pH 6.8), 0.2 mM PMSF at 4 °C. The pellet was suspended in 1 ml of an extraction solution (300 mM KCl, 5 mM ATP-Mg, 10 mM $MgCl_2$, 0.1 mM DTT and 150 mM phosphate, pH 6.8). After incubation on ice for 60 min, the insoluble fraction was removed by centrifugation at 20,000 × *g* for 15 min. The supernatant was dialyzed overnight against 1000 vol of solution containing 10 mM KCl, 0.1 mM DTT and 10 mM Tris-HCl (pH 7.2). Protein concentration was determined according to the Bradford method using albumin as a standard. Tissue lysates were prepared by grinding with liquid nitrogen, and boiled in SDS-sample buffer (50 mM Tris-HCl, 2% SDS, 100 mM DTT and 100 mM NaCl, pH 6.8). Two hundred nanograms of total lysate or 20 ng of purified mouse myosin was separated on a 7–14% gradient SDS gel, and the protein was transferred to polyvinylidene fluoride (PVDF) membranes (IPVH00010, Millipore). After blocking, the blots were incubated with sera from transgenic mice at 1:10,000 dilution, followed by incubation with HRP-conjugated sheep anti-mouse IgG (NA931V, GE Healthcare) at 1:20,000 dilution. Signals were developed using SuperSignal West Femto Maximum Sensitivity Substrate (Thermo Scientific).

3. Results

3.1. Generation of transgenic mice expressing human AIRE from APCs in the thymus and periphery

In order to achieve discrimination between Aire protein expressed transgenically and that expressed endogenously in mice, we expressed human AIRE (huAIRE) under control of the MHC-II promoter: huAIRE and endogenous mouse Aire protein can be independently monitored using mAbs specific for each by flow-cytometric analysis and immunohistochemistry. Four independent Tg lines (huAIRE-Tg lines 2m9L, 1m4L, 20P and 8 L) expressing huAIRE in the thymus on a NOD background were established, and three lines – except for line 20P which did not breed well – were analyzed in detail. $huAIRE^+$ cells were located predominantly in the medulla, with lower numbers in the cortex (Fig. S1A). Because we utilized the MHC-II promoter, B cells and DCs also expressed

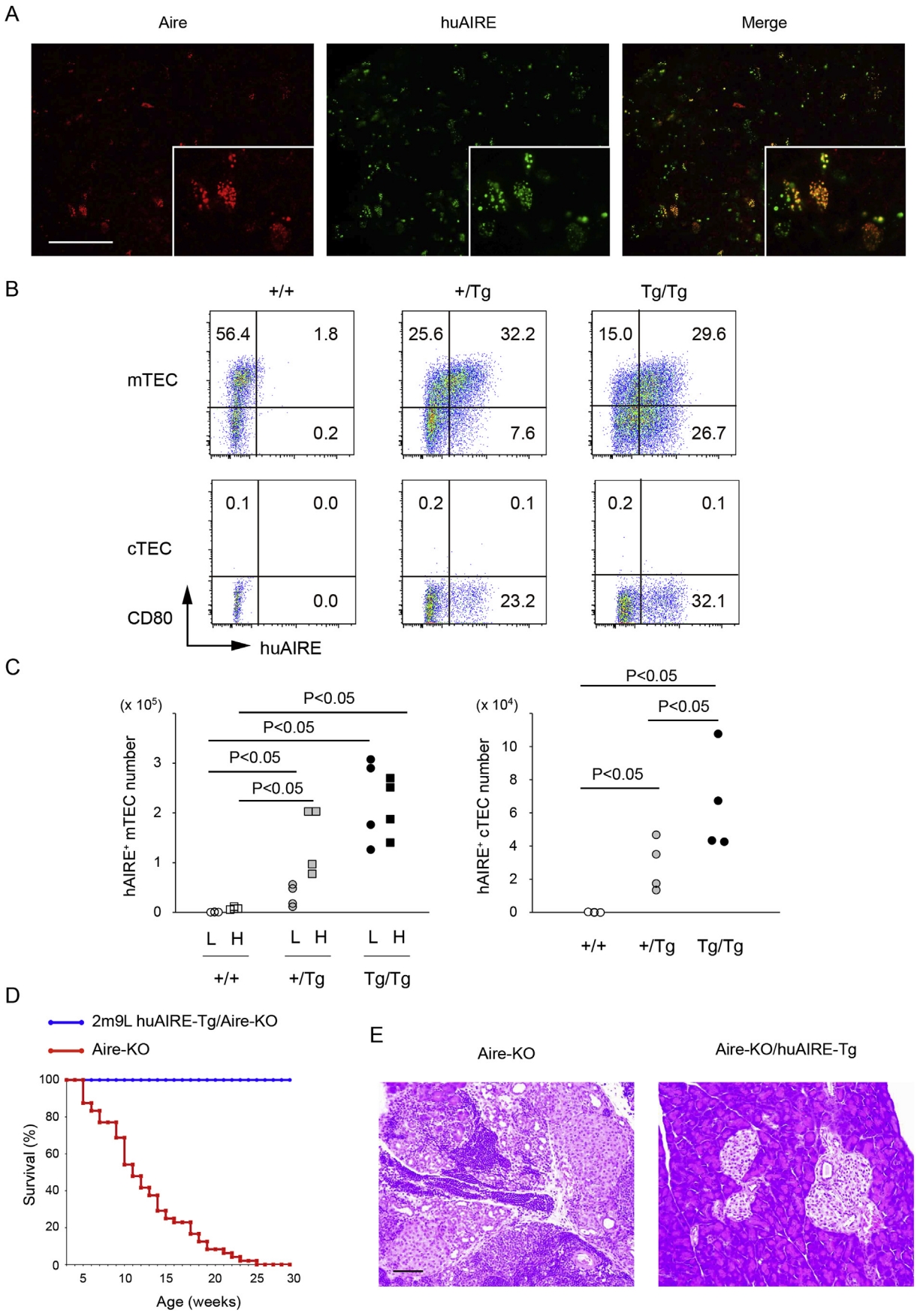

Fig. 1. Functional properties of huAIRE additively expressed in mTECs. (**A**) Co-localization of endogenous mouse Aire and huAIRE in the thymus from heterozygous 2m9L huAIRE-Tg. Insets are enlargements of parts of each staining. Scale bar: 50 μm. (**B**) Flow-cytometric analysis of huAIRE expression by mTECs (gated for CD45$^-$EpCAM$^+$UEA-1$^+$ cells; *upper*) and by cTECs (CD45$^-$EpCAM$^+$Ly51$^+$ cells; *lower*). (**C**) Absolute numbers of huAIRE$^+$ mTECs (L, mTEClow; H, mTEChigh, *left*) and huAIRE$^+$ cTECs (*right*). (**D**) Rescue of the lethal phenotype of Aire-deficient NOD mice ($n = 48$) by crossing with heterozygous 2m9L huAIRE-Tg ($n = 35$). $P < 0.001$, Log-Rank test. (**E**) Aire-deficient NOD mice showed acinar cell destruction with sparing of the islets of Langerhans (*left*), whereas Aire-deficient NOD mice crossed with 2m9L huAIRE-Tg (Aire-KO/huAIRE-Tg) showed no acinar cell destruction characteristic of NOD mice lacking Aire (*right*). Scale bar: 100 μm.

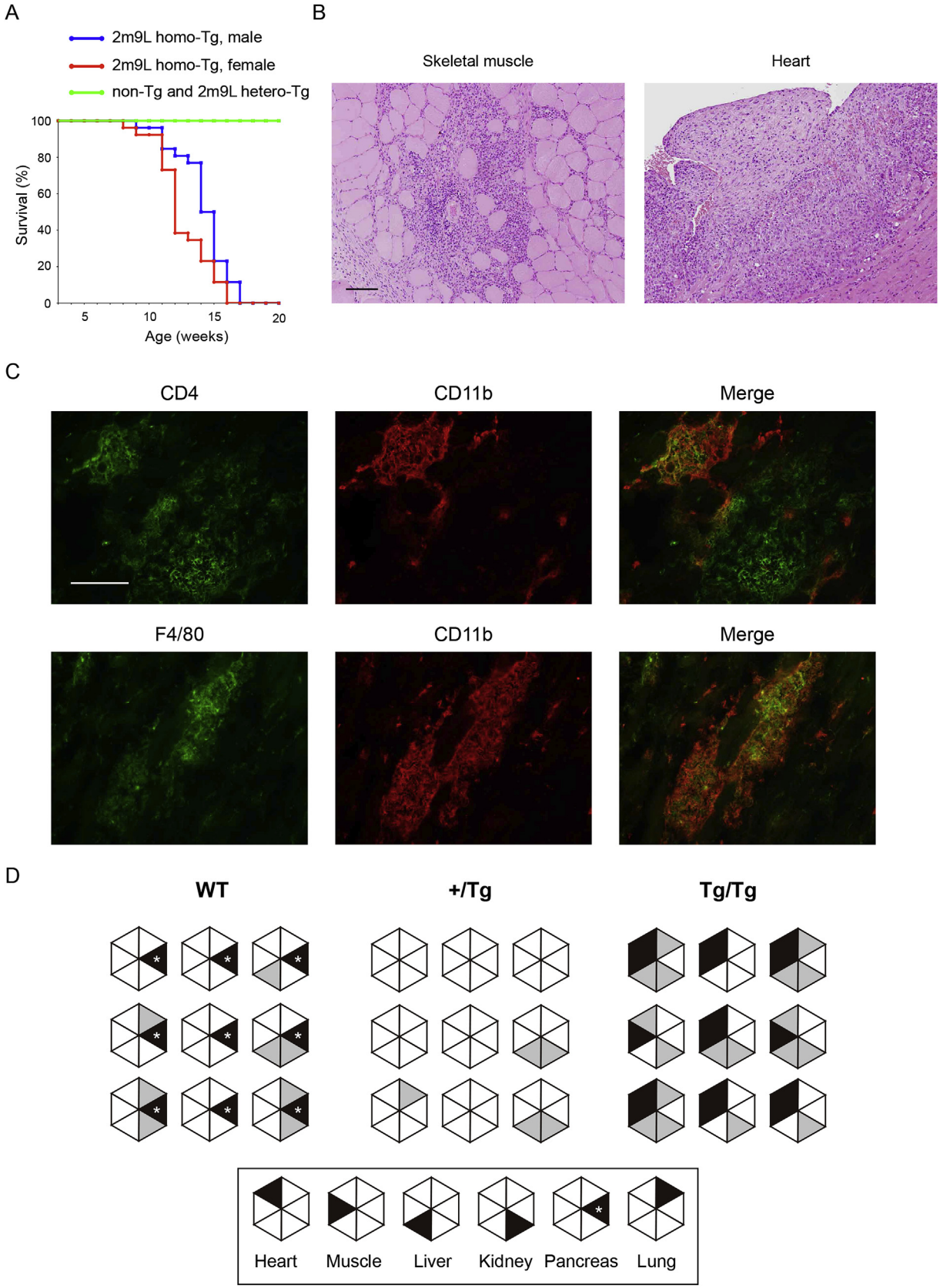

Fig. 2. Paradoxical development of polymyositis-like autoimmunity by additive expression of huAIRE. (**A**) Premature death of homozygous 2m9L huAIRE-Tg (male, $n = 26$; female, $n = 26$). Female homozygous huAIRE-Tg (red line) died more quickly than male homozygous huAIRE-Tg (blue line). $P = 0.012$, Log-Rank test. Survival curve of the mixture of wild-type non-Tg (male, $n = 16$; female, $n = 15$) and heterozygous huAIRE-Tg (male, $n = 55$; female, $n = 43$) are shown in green. (**B**) Polymyositis-like autoimmunity in skeletal muscle and heart in homozygous 2m9L huAIRE-Tg. Scale bar: 100 μm. (**C**) Immune cells infiltrating into the skeletal muscle were composed predominantly of $CD4^+$ T cells and $CD11b^+F4/80^+$ inflammatory cells revealed by immunohistochemistry. Scale bar: 200 μm. (**D**) Pathological changes in the indicated organs from wild-type (WT), heterozygous (+/Tg) and homozygous 2m9L huAIRE-Tg (Tg/Tg) assessed with H.E. staining. Nine mice at 10–20 weeks of age from each group were evaluated. Black, severe; gray, mild; white, none. *, lymphoid cell infiltration into pancreatic β-islets from wild-type NOD mice.

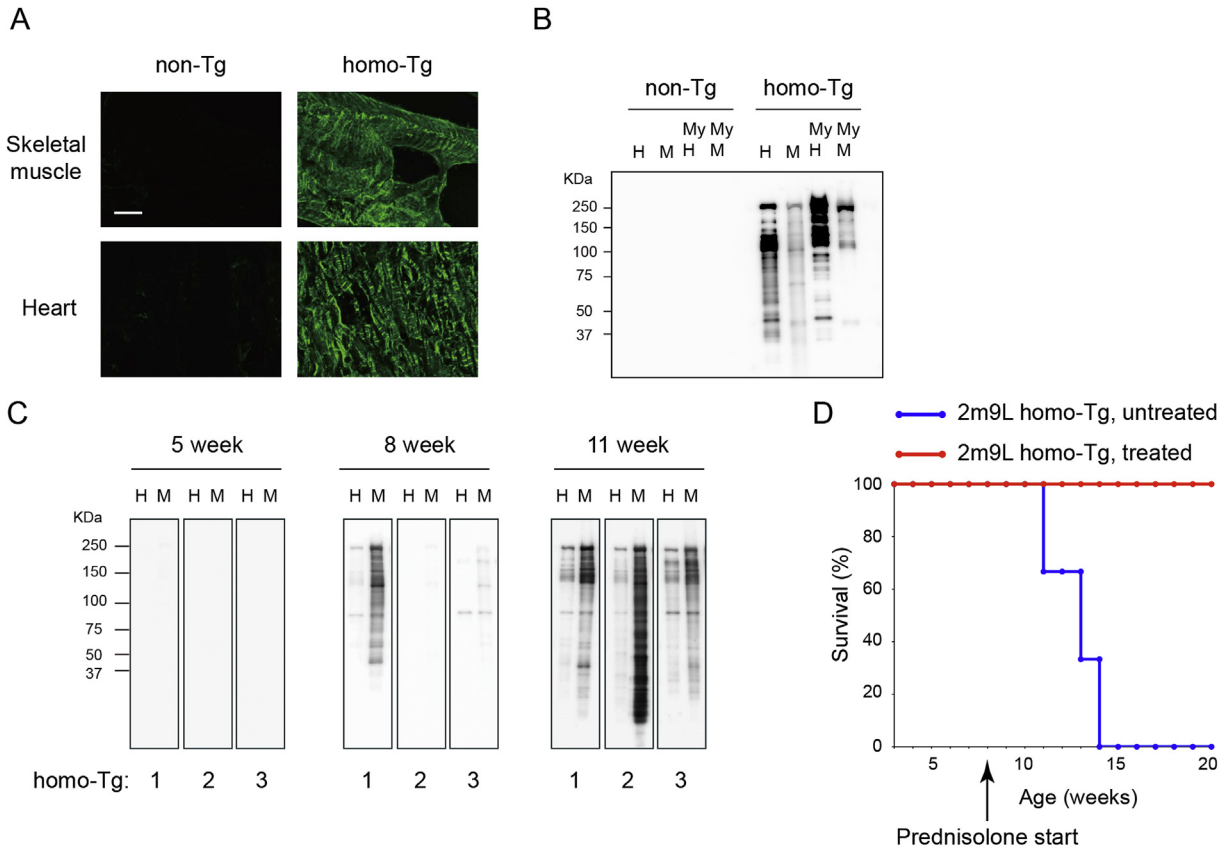

Fig. 3. Production of autoantibodies against muscle tissues in huAIRE-Tg. (**A**) Detection of autoantibodies in the sera from homozygous 2m9L huAIRE-Tg against skeletal muscle and heart using immunohistochemistry. Scale bar: 10 μm. (**B**) Western blot analysis using protein extract from heart (H), skeletal muscle (M), and crude myosin prepared from heart (My H) or from skeletal muscle (My M). Sera obtained from non-Tg (*left*) and homozygous huAIRE-Tg (*right*) were examined for their reactivity. (**C**) Sequential analysis of the production of autoantibodies against heart (H) and skeletal muscle (M). Sera were harvested from peripheral blood of the same homozygous 2m9L huAIRE-Tg (i.e., mouse 1, 2 and 3) at the indicated ages. (**D**) Supplementation of drinking water with prednisolone starting from 8 weeks of age [5 mg/kg/day ($n = 4$) or 1 mg/kg/day ($n = 2$)] prevented the lethality of homozygous 2m9L huAIRE-Tg ($n = 6$ in total). All the control mice without prednisolone treatment died prematurely ($n = 3$). $P < 0.01$, Log-Rank test.

huAIRE. Assessment of huAIRE expression in peripheral blood showed that line 2m9L had ~30% huAIRE$^+$ B cells, followed by ~8% in line 1m4L and ~2% in line 8 L (Fig. S1B). This variation in the level of huAIRE expression was correlated with the expression level of huAIRE in the thymus (Figs. S1A and S1B).

Detailed immunohistochemistry of mTECs using huAIRE-specific polyclonal Ab and mouse Aire-specific mAb in line 2m9L showed that approximately three-quarters of the huAIRE$^+$ cells contained typical nuclear dots of huAIRE, in which endogenous mouse Aire was completely co-localized (Fig. 1A). The other one-quarter of the huAIRE$^+$ cells expressed huAIRE as a single to a few larger nuclear dots within an mTEC, in which mouse Aire was scarcely co-expressed. In two other lines (1m4L and 8 L) which showed lower levels of huAIRE expression than line 2m9L, nuclear dots of huAIRE and endogenous mouse Aire showed an almost completely overlapped distribution in the thymus (data not shown).

Flow-cytometric analysis of mTECs from line 2m9L showed that, in heterozygous huAIRE-Tg (+/Tg), huAIRE was expressed predominantly by mature mTECs with CD80^{high} expression (mTEC^{high}) (Fig. 1B, *upper*: gating strategy for each TEC fraction is shown in Fig. S2). When mice were bred onto homozygosity for the transgene (Tg/Tg), we observed more huAIRE$^+$ mTECs, half of which were from the CD80^{low} population (Fig. 1B, *upper* and 1C, *left*). cTECs from heterozygous 2m9L huAIRE-Tg also expressed huAIRE, and homozygous 2m9L huAIRE-Tg had more huAIRE$^+$ cTECs (Fig. 1B, *lower* and 1C, *right*).

Importantly, premature death due to the severe autoimmune phenotypes seen in NOD mice lacking Aire (i.e., massive acinar cell destruction in the pancreas and severe pneumonitis) [18] was completely abrogated by crossing with each of the three huAIRE-Tg lines [depicted for line 2m9L in Fig. 1D (for survival) and Fig. 1E (for pancreatic pathology)]. Furthermore, Aire-deficient heterozygous huAIRE-Tg (Aire-KO/heterozygous huAIRE-Tg) derived from lines 1m4L and 8 L, but not 2m9L (see the following section of "3.2. Development of muscle-specific autoimmunity in huAIRE-Tg"), developed diabetes similarly to wild-type NOD (data not shown), suggesting that huAIRE can compensate for the loss of endogenous mouse Aire. Thus, transgenic huAIRE expressed by MHC-II$^+$ cells is immunologically competent and physiologically relevant to the roles of endogenous mouse Aire.

All three huAIRE-Tg lines had small thymi in comparison with their littermates (depicted for 2m9L huAIRE-Tg in Fig. S3A), as reflected by the reduced numbers of total thymocytes, CD4$^+$ T cells and CD8$^+$ T cells (depicted for heterozygous 2m9L huAIRE-Tg in Fig. S3B, *left* and S3C). Although the CD4/CD8 ratio of thymocytes was grossly normal in heterozygous huAIRE-Tg in a polyclonal setting (Fig. S3D), the absolute number of thymic Tregs was decreased in homozygous 2m9L huAIRE-Tg, but not in heterozygous huAIRE-Tg (Fig. S3E, *left*). In the spleen, the number of T cells, but not B cells, was decreased in a gene-dosage-dependent manner (Fig. S3F), although the absolute numbers of Tregs were retained

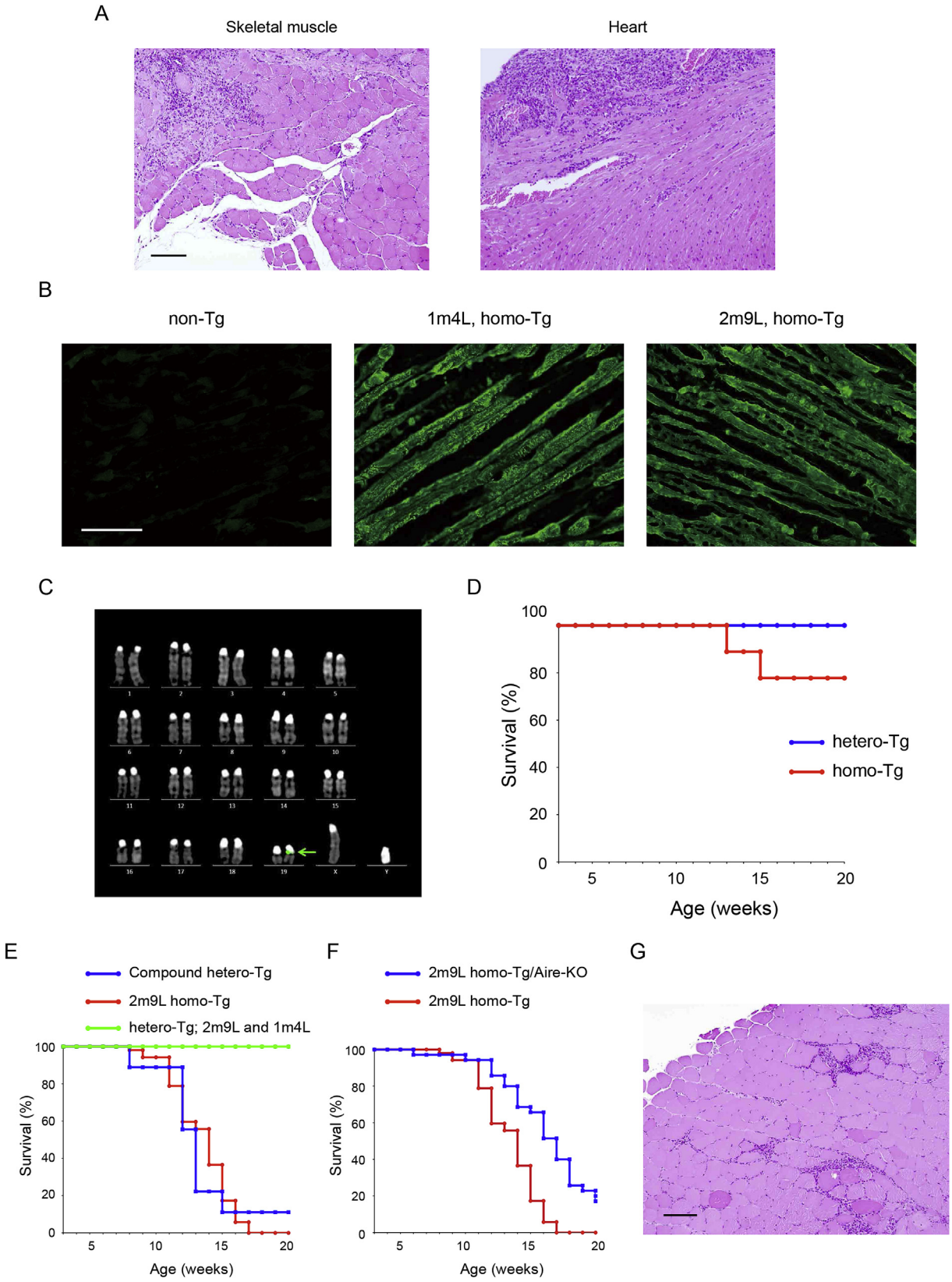

Fig. 4. Gene-dosage effect of huAIRE in autoimmune pathogenesis. (**A**) Polymyositis-like autoimmunity in skeletal muscle and heart from another homozygous huAIRE-Tg line of 1m4L. Scale bar: 100 μm. (**B**) Autoantibody production against skeletal muscle in homozygous 1m4L huAIRE-Tg. Sera from non-Tg and homozygous 2m9L huAIRE-Tg served as negative and positive controls, respectively. Scale bar: 200 μm. (**C**) FISH analysis using huAIRE cDNA revealed transgenic insertion into chromosome 19. The green arrow indicates the signal of the hybridized probe. (**D**) Premature death of homozygous 1m4L huAIRE-Tg. Survival of heterozygous 1m4L huAIRE-Tg ($n = 18$) and homozygous 1m4L huAIRE-Tg ($n = 9$) was monitored. (**E**) Premature death of compound heterozygous huAIRE-Tg between line 2m9L and line 1m4L ($n = 9$). One surviving compound heterozygous huAIRE-Tg showed the typical polymyositis-like pathology together with production of anti-muscle autoantibody upon autopsy. Survival of heterozygous huAIRE-Tg from line 2m9L ($n = 104$) and from line 1m4L ($n = 5$) was monitored, and the results were mixed together (green). Homozygous 2m9L huAIRE-Tg were adapted from Fig. 2A that included both females and males ($n = 52$). $P = 0.831$, Log-Rank test for homozygous 2m9L huAIRE-Tg vs. 2m9L-1m4L compound heterozygous huAIRE-Tg. (**F**) Prolongation of survival of homozygous 2m9L huAIRE-Tg by deleting endogenous mouse Aire ($n = 35$). $P < 0.001$, Log-Rank test. Homozygous 2m9L huAIRE-Tg sufficient for endogenous mouse Aire (red) served as a control (adapted from **E**: $n = 52$). (**G**) Polymyositis-like autoimmunity in homozygous 2m9L/Aire-deficient NOD mice. Scale bars: 100 μm.

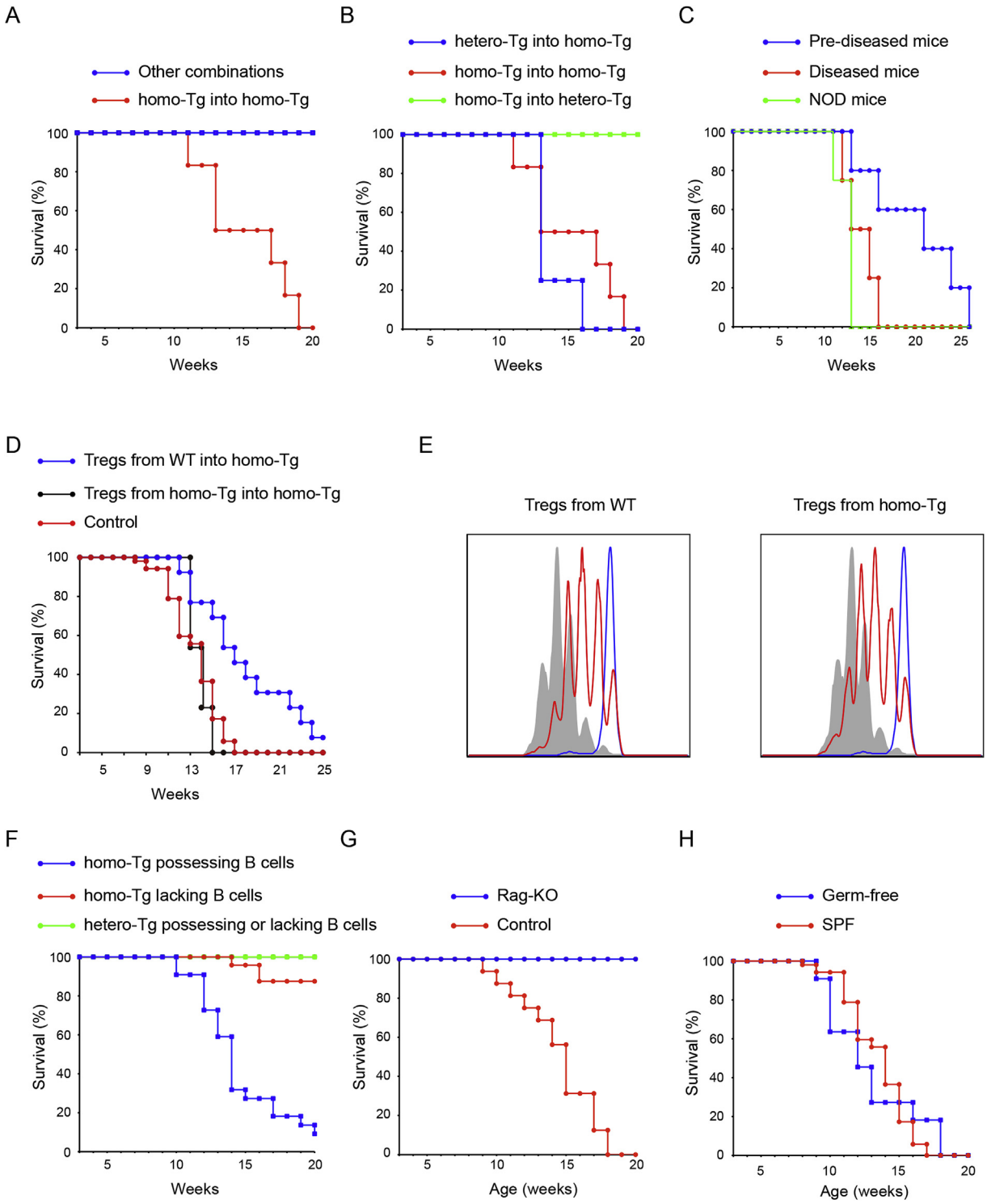

Fig. 5. Cellular mechanisms underlying the development of muscle-specific autoimmunity caused by additive expression of huAIRE. (**A**) Polymyositis-like pathology developed only when both BM donors and recipients were homozygous huAIRE-Tg ($n = 6$) (red), whereas other combinations showed no disease: survival of mice (non-Tg into non-Tg, $n = 5$; non-Tg into homozygous 2m9L huAIRE-Tg, $n = 6$; homozygous 2m9L huAIRE-Tg into non-Tg, $n = 4$) were mixed together (blue). $P < 0.01$, Log-Rank test. (**B**) BM from heterozygous huAIRE-Tg developed the disease when transferred into homozygous huAIRE-Tg ($n = 4$), similarly to the homozygous huAIRE-Tg transferred with BM from homozygous huAIRE-Tg (adapted from **A**: $n = 6$). BM from homozygous huAIRE-Tg did not develop the disease when transferred into heterozygous huAIRE-Tg ($n = 6$) (green). $P < 0.01$, Log-Rank test. (**C**) Development of polymyositis-like pathology by transfer of splenic T cells from homozygous 2m9L huAIRE-Tg into NOD.scid mice. NOD.scid mice received splenic T cells from homozygous huAIRE-Tg already exhibiting the obvious disease phenotype ($n = 4$) or before the onset of disease (both approximately 10 week-old) ($n = 5$), or splenic T cells from wild-type NOD mice ($n = 4$). NOD.scid mice that had received splenic T cells from wild-type NOD mice died due to diabetes, and were free of polymyositis-like pathology upon autopsy. T cells isolated from the diseased mice induced lethality due to polymyositis-like autoimmunity more quickly than those isolated from mice that had not apparently developed the disease. $P < 0.05$, Log-Rank test. (**D**) Ability of Tregs to suppress the autoimmune pathology was examined *in vivo* by transferring Tregs isolated from the spleen of wild-type NOD mice (blue: $n = 13$) or from homozygous 2m9L huAIRE-Tg (black: $n = 13$) into homozygous 2m9L huAIRE-Tg recipients. No prolongation of recipient survival was observed when Tregs isolated from homozygous 2m9L huAIRE-Tg were used, in comparison with those from untreated homozygous 2m9L huAIRE-Tg (red: $n = 52$, adapted from Fig. 2A). $P < 0.001$, Log-Rank test. (**E**) *In vitro* suppression assay showed that the suppressive activity of Tregs from wild-type NOD was indistinguishable from that of Tregs from

(Fig. S3E, *right*). The *in vivo* and *in vitro* function of Tregs from homozygous 2m9L huAIRE-Tg is described in the section "3.4. Cellular mechanisms underlying the development of muscle-specific autoimmunity caused by additive expression of AIRE" below.

3.2. Development of muscle-specific autoimmunity in huAIRE-Tg

During the generation of homozygous huAIRE-Tg for each line, we unexpectedly observed body weight loss followed by premature death of all homozygous huAIRE-Tg from line 2m9L (and also a small number from line 1m4L; see below), both females and males (Fig. 2A). Pathological examination demonstrated marked infiltration of immune cells into skeletal muscle throughout the body in all of the homozygous huAIRE-Tg (Fig. 2B, *left*). Immunohistochemical analyses showed that these infiltrating cells were predominantly $CD4^+$ T cells and $CD11b^+F4/80^+$ inflammatory cells (Fig. 2C). In most cases, we also observed severe pathological changes in the heart (Fig. 2B, *right*), and we suspected that the premature sudden death in homozygous 2m9L huAIRE-Tg had been due to heart failure and/or arrhythmia.

We also observed lymphoid-cell infiltrations in other organs such as kidney (8 out of 9 mice examined), liver (5 out of 9 mice) and lung (3 out of 9 mice) from homozygous 2m9L huAIRE-Tg, but not from heterozygous huAIRE-Tg (Fig. 2D). However, the degree of infiltration of immune cells in these organs was much milder than that in muscle and heart (data not shown). Of note, both heterozygous and homozygous huAIRE-Tg showed no pancreatic pathology, in marked contrast to control littermates (Fig. 2D; histology is not shown, but was similar to that from Aire-KO/huAIRE-Tg shown in Fig. 1E). Consistent with this finding, heterozygous 2m9L huAIRE-Tg showed complete resistance to diabetes development ($n = 54$), whereas female mice from the other two lines developed diabetes similarly to control littermates [55.6% in line 1m4L ($n = 9$); 100% in line 8 L ($n = 5$); 64.7% in non-Tg ($n = 17$)] when the cumulative incidence of diabetes development was monitored until 40 weeks of age. The mechanisms underlying the acquisition of resistance to diabetes in line 2m9L are currently unknown, and detailed analyses of this phenotype are now underway. Whether $CD4^+$ T cells specific for insulin are present in heterozygous 2m9L huAIRE-Tg, and how these cells, if present, respond upon challenge with insulin peptide, might be crucial in future investigations.

Because the pathological changes in homozygous 2m9L huAIRE-Tg showed marked similarity to the human autoimmune disorder polymyositis, which affects skeletal muscles predominantly in the limbs, together with heart muscle in severe cases [28], we investigated whether the disease in homozygous 2m9L huAIRE-Tg was due to autoimmunity. First, we examined production of autoantibody against skeletal muscle and heart using immunohistochemistry, and found that sera from all homozygous 2m9L huAIRE-Tg showed reactivity against these tissues, whereas those from heterozygous huAIRE-Tg (data not shown) or non-Tg littermates contained no such autoantibodies (Fig. 3A). Western blot analysis demonstrated major reactivity against a protein of more than 250 kDa, most likely myosin (Fig. 3B) [29]. Indeed, sera from homozygous huAIRE-Tg showed reactivity against purified myosin (Fig. 3B).

The production of autoantibody against skeletal muscle and heart was age-dependent. We found that homozygous 2m9L huAIRE-Tg at five weeks of age produced no detectable autoantibody against these tissues, as examined by Western blotting (Fig. 3C). However, all the mice produced autoantibody by 11 weeks of age upon sequential monitoring of individual mice. Consistent with disease autoimmunity, supplementation of drinking water with prednisolone completely abolished their premature death (Fig. 3D).

Of note, polymyositis-like autoimmunity in homozygous 2m9L huAIRE-Tg described above was not confined to a NOD background. Instead, similar phenotypes were observed after backcrossing 2m9L huAIRE-Tg onto a Balb/c background for more than four generations (data not shown). Thus, the effect of the augmented AIRE/Aire expression *in vivo* was evident in broader experimental settings.

3.3. Development of muscle-specific autoimmunity is due to the gene-dosage effect of huAIRE/Aire

Although we observed the development of polymyositis-like autoimmunity from line 2m9L only when the transgene was homozygous and not heterozygous, this was not due to homozygous disruption of the genomic region important for regulating self-tolerance through transgenic insertion. Rather, the disease was due to the gene-dosage effect of huAIRE/Aire for the following reasons. First, transgenic insertion in line 2m9L, determined by Southern blot analysis [revealing that the transgenic integration into the genome was at a single site (Figs. S4A and S4B)] and by the adaptor-ligated PCR method [30], was shown to occur in an intergenic region of chromosome 16qC4, where no functional genes have been recorded (Fig. S4C). Second, we observed development of muscle-specific autoimmunity from another huAIRE-Tg line, 1m4L, when bred onto homozygous mice (Fig. 4A and B): FISH analysis showed that the transgene was located on chromosome 19qB in line 1m4L (Fig. 4C). In contrast to line 2m9L, however, only ~20% of homozygous 1m4L huAIRE-Tg manifested the disease (Fig. 4D). Therefore, we assume that the amount of huAIRE/Aire protein expressed in homozygous 1m4L huAIRE-Tg was close to the threshold required for inducing the disease. Third and most convincingly, we observed development of the disease in 100% of animals produced by crossing line 2m9L with 1m4L in order to generate compound heterozygosity (Fig. 4E), thus excluding the possibility that the phenotype was due to disruption of the particular genomic loci by transgenic insertion. Finally, homozygous 2m9L huAIRE-Tg lacking endogenous mouse Aire generated by crossing homozygous 2m9L huAIRE-Tg onto Aire-deficient NOD mice showed a significant delay of premature death in comparison with homozygous 2m9L huAIRE-Tg/Aire-sufficient NOD mice (Fig. 4F), although muscle-specific pathological changes remained (Fig. 4G). These results strongly suggested that tissue-specific autoimmunity was paradoxically induced when an excess amount of autoimmune-

homozygous 2m9L huAIRE-Tg. Dilution of the CFSE from the responding cells (red lines) was monitored after mixing with Tregs isolated from wild-type NOD mice (*left*) or homozygous 2m9L huAIRE-Tg (*right*) at a 2:1 ratio in the presence of CD3/CD28 antibody beads. Gray shadows represent the cell division of $CD4^+$ T cells without admixed Tregs, and blue lines represent that of $CD4^+$ T cells alone without CD3/CD28 stimulation. One representative experiment from a total of three repeats is shown. (**F**) Homozygous huAIRE-Tg lacking B cells ($Ighm^{-/-}$) (red; $n = 24$) survived significantly longer than control homozygous huAIRE-Tg ($Ighm^{+/+}$ and $Ighm^{+/-}$) (blue; $n = 22$). $P < 0.001$, Log-Rank test. Heterozygous huAIRE-Tg sufficient for B cells ($Ighm^{+/-}$) ($n = 5$) or deficient for B cells ($Ighm^{-/-}$) ($n = 13$) developed no disease, and the results of their survival were mixed together (green). (**G**) Homozygous 2m9L huAIRE-Tg deficient for Rag2 did not develop the disease ($n = 12$). Homozygous 2m9L huAIRE-Tg sufficient for Rag2 ($Rag2^{+/+}$ and $Rag2^{+/-}$) ($n = 16$) served as controls. (**H**) Premature death of homozygous 2m9L huAIRE-Tg was observed under germ-free conditions. Survival of homozygous huAIRE-Tg maintained under germ-free ($n = 11$) and specific-pathogen free (SPF) conditions ($n = 52$, adapted from Fig. 2A) was monitored.

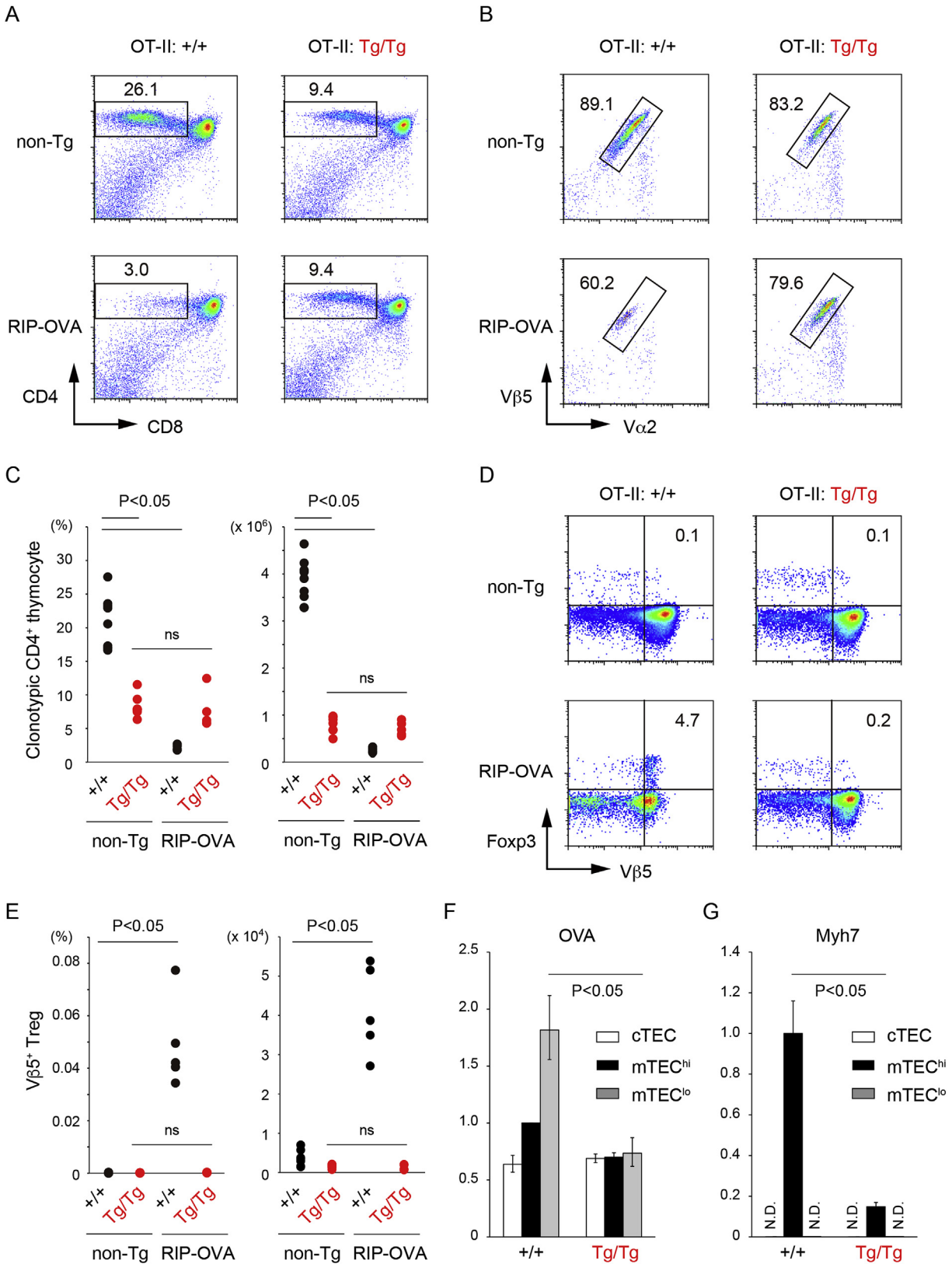

Fig. 6. Defective central tolerance by additive expression of huAIRE. (**A**) Impaired clonal deletion of CD4^{+} OT-II cells in the thymus when crossed with RIP-OVA Tg in homozygous 2m9L huAIRE-Tg. (**B**) After gating for CD4 single-positive T cells in **A**, clonotypic T cells were assessed using anti-Vα2 and anti-Vβ5 mAbs. (**C**) Percentages and absolute numbers of clonotypic T cells shown in **A** and **B**. OT-II: +/+, $n = 9$; Tg/Tg, $n = 7$. OT-II crossed with RIP-OVA Tg: +/+, $n = 5$; Tg/Tg, $n = 5$. ns, not significant. (**D**) Impaired production of antigen-specific Tregs in the thymus by additive expression of huAIRE in OT-II Tg crossed with RIP-OVA Tg. (**E**) Percentages and absolute numbers of clonotypic Tregs shown in **D**. The same animals as those examined in **A-C** were used for the analysis. (**F**) Levels of OVA expression from isolated TEC populations in RIP-OVA Tg on wild-type or homozygous 2m9L huAIRE-Tg background (both on C57BL/6) were examined by real-time PCR. The expression level of *Hprt* was used as an internal control for RNAs. The expression level of OVA in wild-type mTEC^{high} was defined as 1. (**G**) Levels of Myh7 expression from isolated TEC populations from wild-type or homozygous 2m9L huAIRE-Tg (both on NOD) were examined by real-time

regulating huAIRE/Aire protein was present in thymic and peripheral APCs.

3.4. Cellular mechanisms underlying the development of muscle-specific autoimmunity caused by additive expression of AIRE

Our reciprocal BM transfer experiment suggested that both BM-derived cells and non-BM-derived cells expressing huAIRE were required for the development of polymyositis-like autoimmunity in homozygous 2m9L huAIRE-Tg (Fig. 5A). Interestingly, BM from heterozygous 2m9L huAIRE-Tg also induced polymyositis-like autoimmunity when transferred into homozygous 2m9L huAIRE-Tg (Fig. 5B).

The disease was caused by the autoimmune T-cell repertoire in homozygous 2m9L huAIRE-Tg. When purified splenic T-cells isolated from homozygous 2m9L huAIRE-Tg were transferred into immunodeficient NOD.scid mice, all the mice developed polymyositis-like autoimmunity (Fig. 5C) with no pancreatic pathology (data not shown). It was noteworthy that T cells isolated from the diseased mice (Fig. 5C, red line) induced lethality due to polymyositis-like autoimmunity in NOD.scid mice more quickly than those isolated from mice that had not apparently developed the disease (Fig. 5C, blue line). In marked contrast, T cells isolated from control non-Tg NOD mice induced lethality associated with severe diabetes, but not polymyositis-like autoimmunity, in all of the recipient mice (Fig. 5C, green line).

We examined the ability of Tregs to ameliorate the lethal autoimmunity seen in homozygous 2m9L huAIRE-Tg. When we transferred Tregs isolated from the spleen of wild-type NOD mice into homozygous 2m9L huAIRE-Tg, we observed prolongation of survival of the recipient homozygous 2m9L huAIRE-Tg (Fig. 5D, blue line). However, when we transferred Tregs isolated from the spleen of homozygous 2m9L huAIRE-Tg, we did not observe such an effect (Fig. 5D, black line). This was not due to the defect of the general suppressive activity of Tregs from homozygous 2m9L huAIRE-Tg because *in vitro* suppression assay showed no obvious difference in the Treg activity between wild-type NOD mice and homozygous 2m9L huAIRE-Tg (Fig. 5E). Furthermore, the total numbers of Tregs in the periphery remained unchanged in homozygous 2m9L huAIRE-Tg (Fig. S3E, *right*). We speculate that the repertoire of the Tregs produced in the thymus had been changed by additive expression of huAIRE. In this case, we assume that Tregs specific for muscle-specific antigens were not positively selected in the thymic microenvironment due to the altered spectrum of TRAs expressed from mTECs. Consequently, Tregs that were activated by muscle-specific antigens and able to suppress the muscle-specific autoimmune response in periphery might have been missing in homozygous 2m9L huAIRE-Tg.

Transfer of sera from diseased homozygous 2m9L huAIRE-Tg into wild-type NOD mice induced no inflammatory changes in muscle tissues (data not shown), suggesting that the autoantibodies themselves were not pathogenic. Because B cells might play an important role in activation of autoreactive T cells as peripheral APCs, we next investigated whether B cells are required for the disease process by crossing homozygous huAIRE-Tg onto B-cell-deficient NOD mice. B-cell-deficient homozygous huAIRE-Tg showed significantly milder disease with only rare lethality (Fig. 5F). These results suggested that B cells are an important component of muscle-specific autoimmunity, acting primarily as APCs. Consistent with disease autoimmunity, homozygous 2m9L huAIRE-Tg developed no disease when crossed with Rag2-deficient NOD mice (Fig. 5G). The disease occurred under germ-free conditions in this model (Fig. 5H).

3.5. Impaired negative selection and Treg production in the thymic microenvironment additively expressing huAIRE due to altered development of mTECs

We investigated whether additive expression of huAIRE in the thymus altered negative selection. We employed a TCR-transgenic model in which Aire plays an essential role in clonal deletion of T cells specific for a model self-antigen of ovalbumin (OVA) driven by the rat insulin promoter (RIP-OVA Tg) [8,9,31]. For this purpose, we crossed 2m9L huAIRE-Tg onto C57/BL6 for more than ten generations. OVA-specific TCR Tg (OT-II) on a homozygous huAIRE-Tg background showed a reduction in the percentage and number of clonotypic T cells in the thymus (Fig. 6A, *upper* and 6C), suggesting that positive selection was impaired in this setting. When OVA-specific TCR Tg were crossed with RIP-OVA Tg on a non-huAIRE-Tg background, we observed deletion of clonotypic $CD4^+$ T cells in the thymus (Fig. 6A–C). In contrast, when OVA-specific TCR Tg were crossed with RIP-OVA Tg on a homozygous huAIRE-Tg background, deletion of clonotypic $CD4^+$ T cells was not observed (Fig. 6A–C). In this TCR-Tg model, $V\beta5^+$ clonotypic $Foxp3^+$ Tregs in the thymus were generated only when OT-II mice were crossed with RIP-OVA Tg, and we found that homozygous huAIRE-Tg produced almost no clonotypic Tregs in this experimental setting (Fig. 6D and E). Thus, both clonal deletion and production of antigen-specific Tregs in the thymus were impaired in homozygous huAIRE-Tg demonstrated by the TCR-Tg system.

We isolated $CD80^{low}$ immature mTECs ($mTEC^{low}$) and mature $CD80^{high}$ mTECs ($mTEC^{high}$) from RIP-OVA Tg on wild-type and homozygous 2m9L huAIRE-Tg, both on a C57BL/6 background, and measured the levels of OVA expression. OVA expression by $mTEC^{low}$ was reduced in homozygous huAIRE-Tg relative to wild-type mice (Fig. 6F). In contrast, OVA expression by $mTEC^{high}$ was similar between homozygous huAIRE-Tg and wild-type mice, reminiscent of the somewhat retained OVA expression by mTECs lacking Aire [8] or harboring *Nik* mutation [26], despite the fact that clonal deletion of OT-II cells was impaired in both cases.

Because homozygous 2m9L huAIRE-Tg on a NOD background developed autoimmunity against the myosin heavy chain (MyHC) in a polyclonal setting, we examined the expression of cardiac-type MyHC (α-MyHC: Myh6) and skeletal muscle-type MyHC (β-MyHC: Myh7) in TEC populations using real-time PCR. Myh6 transcripts were not detected in any TECs of wild-type NOD, as reported previously [29], or in those from homozygous huAIRE-Tg (data not shown). In contrast, $mTEC^{high}$ from wild-type NOD expressed *Myh7*, and its expression by $mTEC^{high}$ in homozygous huAIRE-Tg was significantly reduced (Fig. 6G), possibly accounting for the impaired clonal deletion of T cells and/or production of Tregs specific for Myh7 in homozygous huAIRE-Tg.

3.6. Global RNA expression pattern of mTECs from huAIRE-Tg

In order to examine the changes in the global transcriptome of

PCR. The expression level of *Hprt* was used as an internal control for RNAs. The expression level of Myh7 in wild-type $mTEC^{high}$ was defined as 1. N.D. not detected. The data are demonstrated by the averages and SEMs obtained from three repeated experiments using mice at two weeks of age with preparing triplicate samples for each experiment for **F** and **G**.

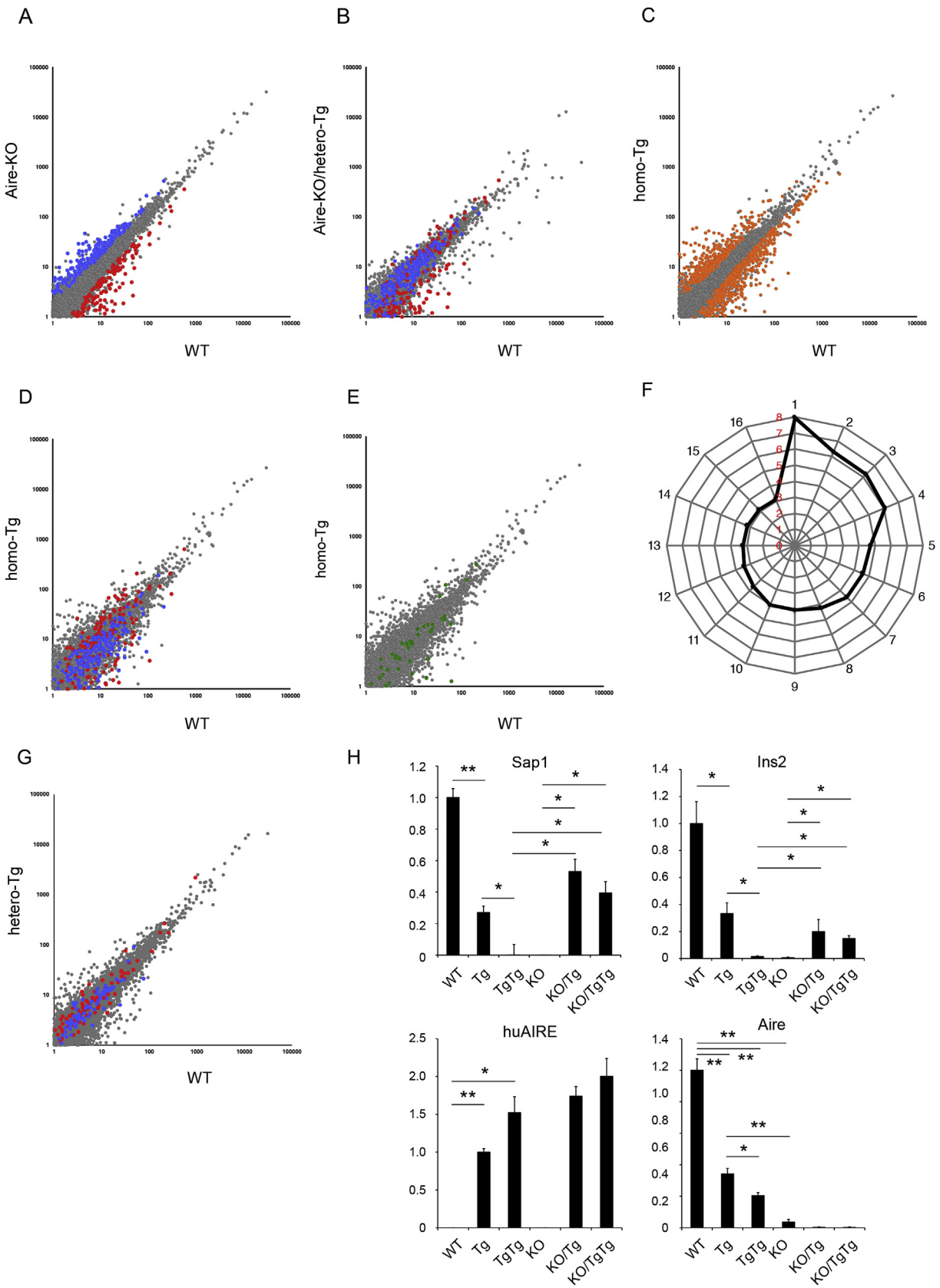

Fig. 7. Global RNA expression and TRA expression from mTECs controlled by huAIRE/Aire. (**A**) Gene expression in wild-type (WT) mTEC^{high} populations versus that in Aire-deficient (Aire-KO) mTEC^{high} populations, showing the 265 Aire-induced genes (red) and 251 Aire-repressed genes (blue). Data were obtained from triplicate samples from each group of mice, and FDR q < 0.05 was defined as significant. (**B**) Gene expression in wild-type mTEC^{high} populations versus that in Aire-deficient heterozygous 2m9L huAIRE-Tg (Aire-KO/hetero-Tg) mTEC^{high} populations. Aire-induced genes (red) and Aire-repressed genes (blue) defined in **A** are colored. (**C**) Gene expression in wild-type mTEC^{high} populations versus that in homozygous 2m9L huAIRE-Tg mTEC^{high} populations. Genes both significantly up-regulated and down-regulated are highlighted in orange. (**D**) Aire-induced

mTECs influenced by the expression of huAIRE, we performed RNA-seq analysis using FACS-sorted mTEC^{high} populations from various strains of mice we established, all on a NOD background. We obtained data from triplicate samples each group of mice, and set FDR q < 0.05 as the level of significance. We first compared the transcriptome between Aire-deficient mice and wild-type mice, and found that 265 genes were down-regulated whereas 251 genes were up-regulated in Aire-deficient mice (Fig. 7A): we defined these genes as "Aire-induced" (in red) and "Aire-repressed" (in blue), respectively. Knowing these Aire-regulated genes, we next compared the transcriptome between Aire-deficient heterozygous 2m9L huAIRE-Tg (Aire-KO/hetero-Tg) and wild-type mice to observe the effect of huAIRE expression in a mouse mTEC environment lacking endogenous mouse Aire. We found that segregation between Aire-induced and Aire-repressed genes was completely cancelled in the presence of huAIRE (Fig. 7B), indicating that huAIRE compensated for the loss of endogenous mouse Aire in mTECs on a global scale. These results are consistent with the fact that crossing huAIRE-Tg onto Aire-deficient mice was able to completely abrogate the lethal phenotype of Aire-deficient mice on a NOD background (Fig. 1D and E).

We then compared the transcriptome between homozygous 2m9L huAIRE-Tg and wild-type mice, and found that there were many differentially expressed genes: 430 genes were up-regulated and 818 genes were down-regulated in homozygous huAIRE-Tg (Fig. 7C, colored in orange). Again, we found no segregation between Aire-induced genes and Aire-repressed genes on a global scale in this setting (Fig. 7D). However, we also noticed that there were many Aire-dependent genes (i.e., genes down-regulated in Aire-deficient mice) that were down-regulated in homozygous 2m9L huAIRE-Tg, including *salivary protein 1* (*Sap1*) and *Ins2* (see the section "3.7. Expression of prototypic Aire-dependent TRAs from mTECs additively expressing huAIRE" below for detailed analysis). Furthermore, we found that several Aire-independent TRAs [32] (Fig. 7E, colored in green) were also down-regulated in homozygous huAIRE-Tg.

Functional annotation of genes up-regulated in homozygous 2m9L huAIRE-Tg compared with wild-type mice using DAVID Bioinformatics Resources 6.7 revealed many immunologically relevant pathways (Fig. 7F): three out of the top five pathways (i.e., 1, response to virus; 2, cell adhesion; 4, immune system process) overlapped with the pathways that were affected by the lack of endogenous mouse Aire (data not shown), suggesting that huAIRE has a common impact with mouse Aire on creation of the transcriptome in the mTEC^{high} population.

We also compared huAIRE-regulated genes in B cells with those in mTEC^{high} in heterozygous 2m9L huAIRE-Tg, and found that they were distinct (Fig. 7G): genes that were up-regulated (in blue) and down-regulated (in red) in B cells did not segregate in a scatter plot generated from mTEC^{high}. These results suggest that Aire regulates gene expression in a cell type-specific manner beyond mTECs, as has been demonstrated for β-cells in the pancreas [33], eTACs [14] and thymic B cells [3].

3.7. Expression of prototypic Aire-dependent TRAs from mTECs additively expressing huAIRE

We then focused on the expression of two prototypic Aire-induced TRA genes, *Sap1* and *Ins2*, from mTECs to see how the loss of Aire or augmented huAIRE/Aire expression affects the expression of these Aire-regulated genes (Fig. 7H). Aire-deficient mice (marked as "KO" in Fig. 7H) showed no detectable levels of these genes, as reported previously [10]. Expression of *Ins2* and *Sap1* was inversely correlated with huAIRE expression (marked as "Tg" and "Tg/Tg"), and homozygous huAIRE-Tg showed no detectable expression of these genes despite the fact that homozygous huAIRE-Tg contained ~10% mTECs expressing endogenous mouse Aire (see Fig. 8A below). Surprisingly, Aire-deficient homozygous huAIRE-Tg (marked as "KO/TgTg") showed expression of these Aire-induced genes, although their expression levels did not reach those of wild-type mice (marked as "WT"). This result was unexpected because both Aire-deficient mice and homozygous huAIRE-Tg showed no detectable levels of *Sap1* and *Ins2* expression. Expression of huAIRE showed the expected patterns from each strain, and the expression levels of endogenous mouse Aire were inversely correlated with those of huAIRE on an endogenous mouse Aire-sufficient background (Fig. 7H, *lower panels*). These results suggested that transcriptional control of these prototypic Aire-induced TRA genes by huAIRE/Aire may not be a direct event. Rather, these Aire-dependent TRAs are induced indirectly by huAIRE/Aire, for example, through control of the maturation process of mTECs [34].

3.8. Altered development of mTECs by additive expression of huAIRE

We thus hypothesized that reduced expression of TRAs such as *Myh7*, *Sap1* and *Ins2* by mTECs from homozygous 2m9L huAIRE-Tg was associated with the altered development of mTECs. We found that the percentage of mTECs expressing endogenous mouse Aire was inversely correlated with huAIRE expression, as examined by flow cytometry (Fig. 8A, *lower left*), and that the absolute number of mTECs expressing endogenous mouse Aire was also decreased in homozygous huAIRE-Tg relative to non-Tg (Fig. 8A, *lower right*). Reduced Aire expression was confirmed by real-time PCR (Fig. 8B). huAIRE-Tg also showed alteration of TEC composition: both cTECs and mTECs were increased in both heterozygous and homozygous huAIRE-Tg (Fig. 8C, *left*) despite their small thymi (Fig. S3A), and the ratios of cTECs to mTECs were altered in homozygous huAIRE-Tg (Fig. 8C, *middle*). The absolute numbers of mTEC^{low}, but not mTEC^{high}, were increased in homozygous huAIRE-Tg (Fig. 8C, *right*). In addition to the expression of Aire-dependent TRAs, an Aire-independent TRA of *C-reactive protein* (*Crp*) from mTEC^{high} was also down-regulated in homozygous huAIRE-Tg (Fig. 8D, *left*), as noted by RNA-seq analysis (Fig. 7E). Consistent with the results

genes (red) and Aire-repressed genes (blue) defined in **A** are highlighted in the scatter plot shown in **C**. (**E**) Approximately 100 representative Aire-independent genes [32] are highlighted in the scatter plot shown in **C**. (**F**) Pathway analysis of genes that were significantly up-regulated in homozygous huAIRE-Tg mTEC^{high} relative to wild-type mTEC^{high} (430 up-regulated genes: FDR <0.05). Selected biological process GO terms and their associated *P* values ($-\log_{10}$) for pathway discovery are shown; 1, response to virus; 2, cell adhesion; 3, negative regulation of transcription from the RNA polymerase II promoter; 4, immune system process; 5, positive regulation of transcription from the RNA polymerase II promoter; 6, covalent chromatin modification; 7, transcription, DNA-templated; 8, positive regulation of osteoblast differentiation; 9, extracellular matrix organization; 10, angiogenesis; 11, regulation of transcription, DNA-templated; 12, microglial cell activation; 13, positive regulation of cell proliferation; 14, growth plate cartilage development; 15, neural tube closure; 16, activation of MAPK activity. (**G**) Comparison of Aire-regulated genes in mTEC^{high} and B cells from heterozygous 2m9L huAIRE-Tg. Red and blue marks indicate down-regulated and up-regulated genes in B cells, respectively, overlaid on a scatter plot generated from mTEC^{high} in heterozygous 2m9L huAIRE-Tg and wild-type mice. (**H**) Expression of Aire-dependent TRAs (*Sap1* and *Ins2*), huAIRE and endogenous mouse Aire from mTEC^{high} was examined by real-time PCR. The level of *Hprt* expression was used as an internal control for RNAs. The expression levels of TRAs and Aire in mTEC^{high} from wild-type mice, and that of huAIRE in mTEC^{high} from heterozygous 2m9L huAIRE-Tg (Tg) were defined as 1. KO/Tg and KO/TgTg denote heterozygous and homozygous 2m9L huAIRE-Tg lacking endogenous mouse Aire, respectively. The data are indicated as averages and SEMs obtained from three repeated experiments using mice at two weeks of age, with preparation of triplicate samples for each experiment. **, $P < 0.01$; *, $P < 0.05$.

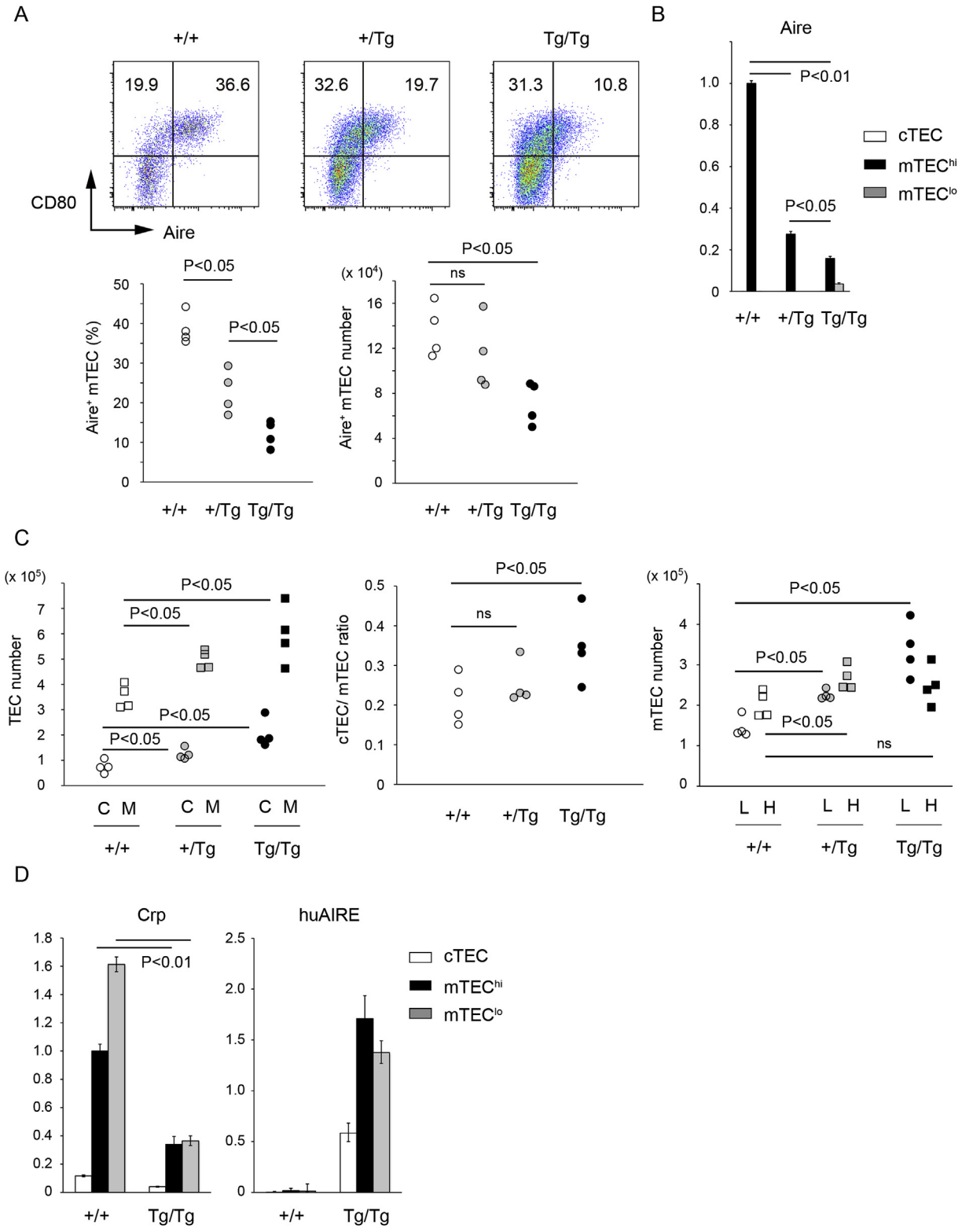

Fig. 8. Gene-dosage-dependent alteration in development of mTECs and TRA expression by additive expression of huAIRE. (**A**) Flow-cytometric analysis of mTECs showed reduced percentages and absolute numbers of endogenous mouse Aire^{+} mTECs by additive expression of huAIRE. (**B**) Levels of expression of endogenous mouse Aire detected by real-time PCR from mTEC^{high} were reduced by additive expression of huAIRE in a dose-dependent manner. Endogenous mouse Aire was not detectable in cTECs in any types of mice. The expression level of *Hprt* was used as an internal control for RNAs. The data are demonstrated by the averages and SEMs obtained from three repeated experiments using mice at two weeks of age with preparing triplicate samples for each experiment. (**C**) Alteration of the composition of TECs was more obvious in homozygous 2m9L huAIRE-Tg than in heterozygous huAIRE-Tg by flow-cytometric analysis. Total numbers of cTECs (C) and mTECs (M) (*left*), ratios between cTECs and mTECs (*middle*), and total numbers of mTEC^{low} (L) and mTEC^{high} (H) (*right*) are shown. (**D**) Expression of *Crp* and huAIRE from isolated TEC populations was examined by real-time PCR. The expression level of *Hprt* was used as an internal control for RNAs. The expression level of TRAs in mTEC^{high} from non-Tg, and that of huAIRE in mTEC^{high} from heterozygous 2m9L huAIRE-Tg were defined as 1. The data are demonstrated by the averages and SEMs obtained from three repeated experiments using mice at two weeks of age with preparing triplicate samples for each experiment.

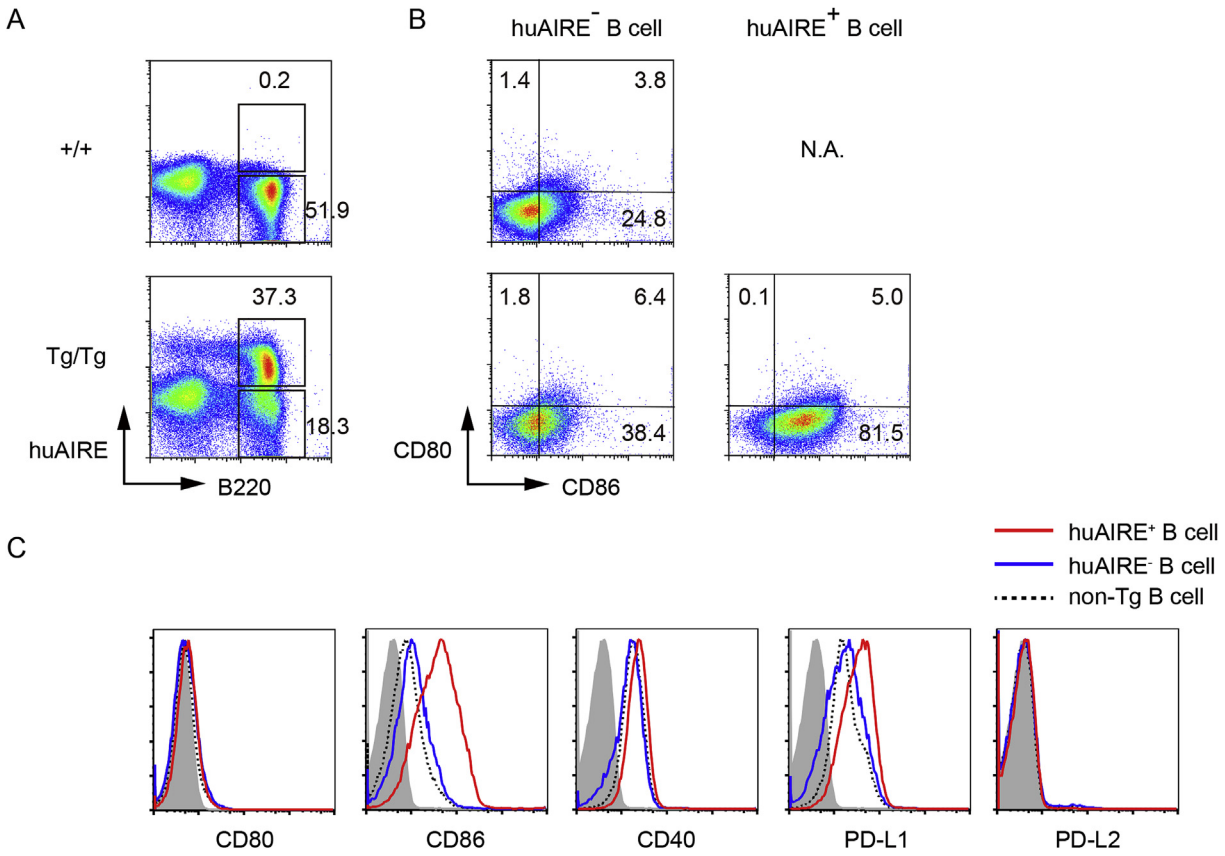

Fig. 9. Augmented expression of costimulatory molecules on peripheral APCs from homozygous 2m9L huAIRE-Tg. (**A**) Splenic B cells from non-Tg and homozygous huAIRE-Tg were examined for their expression of huAIRE. (**B**) Splenic B cells gated for huAIRE$^+$ cells showed higher levels of CD86, but not of CD80, relative to huAIRE$^-$ B cells. One representative experiment from a total of three repeats is shown. N.A. not applicable. (**C**) Expression of CD86 on huAIRE$^+$ B cells was significantly higher compared with that on huAIRE$^-$ B cells in homozygous huAIRE-Tg, or compared with that on B cells from non-Tg. Expression of CD40 and PD-L1 on huAIRE$^+$ B cells was also slightly higher than that on huAIRE$^-$ B cells in homozygous huAIRE-Tg, or that on B cells from non-Tg. Red and blue lines represent huAIRE$^+$ and huAIRE$^-$ B cells from homozygous huAIRE-Tg, respectively. Dotted black lines, B cells from non-Tg; gray shadows, staining with the isotype control.

of flow-cytometric analysis (Fig. 1B), huAIRE was detected in all TEC populations in homozygous huAIRE-Tg (Fig. 8D, *right*).

Because epidermis and mTEC have some common features in terms of their developmental program [23,35,36], we focused on the expression profiles of keratinocyte-related genes in our RNA-seq data set obtained from huAIRE-Tg. Expression of *involucrin*, *loricrin* and *Spink5*, genes expressed from terminally differentiated mTECs, were down-regulated in homozygous huAIRE-Tg (Fig. S5), as demonstrated previously for Aire-deficient mTECs [23]. Many keratinocyte-related genes (e.g., *Krt1*, *Krt2*, *Krt4*, etc.) which have been shown to be down-regulated in Aire-deficient mTECs [35,36], were also down-regulated in those from homozygous huAIRE-Tg. Given that Aire has a role for promoting the differentiation program of mTEC [34], these results suggested that both Aire deficiency and augmented huAIRE/Aire expression had a similar impact on the developmental program of mTECs, creating the defect in their maturation and tolerogenic function such as clonal deletion and Treg production, at least in part through impairment of TRA expression.

3.9. Augmentation of the costimulatory pathway by expression of huAIRE in peripheral APCs

In addition to the high expression of huAIRE in the thymus, its expression in peripheral APCs was necessary for the development of polymyositis-like autoimmunity (Fig. 5A), in which B cells play an important role (Fig. 5F). We found that more than 50% of splenic B-cells expressed huAIRE in homozygous 2m9L huAIRE-Tg (Fig. 9A). Interestingly, huAIRE$^+$ B-cells from homozygous huAIRE-Tg expressed significantly higher levels of CD86 and slightly higher levels of CD40 and PD-L1 compared with those in huAIRE$^-$ B-cells (Fig. 9B and C), whereas expression of both CD80 and PD-L2 was indistinguishable between huAIRE$^+$ and huAIRE$^-$ B-cells. These results suggested that augmented expression of costimulatory molecules in peripheral APCs plays a role in the breakdown of peripheral tolerance in this model, although we cannot rule out the possibility that these changes might be secondary to the development of muscle-specific autoimmunity.

4. Discussion

Through transgenic technology, enforced expression of single TRAs that are not detectable in mTECs has been shown to render autoimmune-prone mice tolerant to the corresponding TRAs, thus curing their autoimmunity [29,37]. Because the primary action of Aire has been suggested to promote TRA expression by mTECs [10] and to functionally inactivate CD4$^+$ T cells in the periphery [13], it was striking that additive expression of huAIRE in mTECs and peripheral APCs resulted in paradoxical impairment of TRA expression and augmentation of costimulatory expression, respectively. Our results highlight the importance of coordinated action between central tolerance and peripheral tolerance under the common control of Aire.

The present results strongly suggest that level of Aire

expression needs to be tightly controlled to prevent autoimmunity: even the transcription factor of Aire necessary for establishing self-tolerance can become harmful once its expression has become excessive. In this regard, the connection between the increased frequency of autoimmune diseases in Down syndrome and AIRE merits attention: Down syndrome is caused by trisomy of chromosome 21, in which *AIRE* is located. Although the levels of AIRE expression have been inconsistent among studies, all reports have attributed the propensity for autoimmunity in Down syndrome to the altered levels of expression of TRAs controlled by AIRE [38–40]. Interestingly, two groups have reported that expression of both AIRE and TRAs were, in fact, decreased in Down syndrome [38,40]. One possible explanation for this is that reduced AIRE expression might be a result of perturbation of mTEC development caused by the gene-dosage effect of AIRE due to chromosome 21 trisomy, as we observed for huAIRE-Tg. Consistent with this idea, structural alternations of the thymus have been noted in all the studies of Down syndrome [38–40]. Thus, it is possible that dysfunction of AIRE is caused not only by *AIRE* mutation but also by the altered gene dosage of *AIRE*. Accordingly, it would also be interesting to determine whether AIRE is overexpressed in some patients with thymomas that are associated with polymyositis and/or myocarditis [41–43], in view of their phenotypic similarities with homozygous 2m9L huAIRE-Tg described in this study.

Although thyroiditis, hypothyroidism and type 1 diabetes, but not polymyositis, are common in Down syndrome [44–46], the phenotypic difference between the autoimmune disease seen in Down syndrome and polymyositis-like autoimmunity we observed in homozygous huAIRE-Tg may not exclude the common mechanisms underlying the autoimmune pathogenesis in the two situations. This is supported by the fact that AIRE deficiency in humans and that in Aire-deficient mice have little overlap with regard to the target-organ specificity of autoimmune disease [10,47–49]. So far, a link between molecular targets of autoimmune attack and TRAs down-regulated in mTECs from patients with Down syndrome has not been reported [38–40]. Similarly, although we found that expression of *Myh7*, a muscle autoantigen, was down-regulated in mTECs from homozygous 2m9L huAIRE-Tg (Fig. 6G), a general link between the spectrum of TRAs shaped by altered huAIRE/Aire expression and the target-organ specificity of autoimmune attack awaits further study.

We utilized human AIRE instead of mouse Aire for augmentation of huAIRE/Aire expression because this enabled us to distinguish transgenically expressed huAIRE from endogenous mouse Aire. It is noteworthy that huAIRE was able to compensate for the loss of endogenous mouse Aire: transgenic huAIRE expression abrogated the lethal phenotype of Aire-deficient NOD mice (Fig. 1D and E), clearly indicating that huAIRE is functional in mice. Our transcriptomic analysis of mTECs from Aire-KO/huAIRE-Tg also supported this view: expression of huAIRE was able to largely normalize the transcriptome alteration caused by the deficiency of endogenous mouse Aire on a global scale (Fig. 7B).

Nevertheless, it is noteworthy that there were many Aire-induced TRAs, such as *Sap1* and *Ins2*, that were almost absent from mTECs in homozygous huAIRE-Tg: this was observed despite the fact that homozygous huAIRE-Tg contained ~10% mTECs expressing endogenous mouse Aire (Fig. 8A). We think that this was not due to inhibition of endogenous mouse Aire by huAIRE because homozygous huAIRE-Tg either deficient for or sufficient for endogenous mouse Aire never showed the phenotypes of Aire deficiency on a NOD background (i.e., massive acinar cell destruction in the pancreas and severe pneumonitis) [18] (data not shown). We assume that both Aire deficiency and additive expression of huAIRE caused the defect in mTEC maturation that would result in altered TRA expression [34]. Consistent with this idea, crossing Aire-deficient mice with homozygous huAIRE-Tg (Aire-KO/homozygous huAIRE-Tg), that would alleviate the extreme effect of either complete absence of Aire (in Aire-deficient mice) or excess huAIRE/Aire (in homozygous huAIRE-Tg) on mTEC maturation, led to recovery of the expression of these Aire-dependent TRAs (Fig. 7H). Accordingly, homozygous 2m9L huAIRE-Tg lacking endogenous mouse Aire (Aire-KO/homozygous huAIRE-Tg) showed a significant delay of premature death in comparison with homozygous huAIRE-Tg possessing endogenous mouse Aire (Fig. 4F).

Because we utilized the MHC-II promoter to express huAIRE in thymic and peripheral APCs, cTECs from huAIRE-Tg also harbored huAIRE, although to a lesser extent compared with that from mTECs. However, we think that the contribution of huAIRE$^+$ cTECs to the development of muscle-specific autoimmunity in homozygous huAIRE-Tg is rather minimal because a semi-knockin strain of NOD-background mice expressing mouse Aire under control of the promoter of β5t, a thymoproteasome expressed exclusively in the cortex, did not confer transcriptional expression of either Aire-dependent or Aire-independent TRAs from cTECs [25]. The thymic microenvironment harboring Aire$^+$ cTECs also showed no obvious alteration of positive selection (i.e., usage of TCRα- and TCRβ-chains for CD4 single-positive and CD8 single-positive thymocytes) [25], suggesting that generation of the muscle-specific autoimmune T cell repertoire in homozygous huAIRE-Tg is most likely attributable to the phenotypically altered mTECs caused by huAIRE expression.

Although expression of huAIRE resulted in altered development of mTECs with defective expression of a wide variety of TRAs, it remains unknown why the breakdown of self-tolerance culminated in muscle destruction. In this connection, it is interesting to note that transgenic mice expressing HLA-DQ8 (DQA1*0301/DQB1*0302), a human MHC-II subtype associated with type 1 diabetes, simultaneously lacking endogenous mouse MHC (I-Aβ) on a NOD background developed autoimmune myocarditis but not polymyositis, although autoantibodies produced in the mice reacted with both the cardiac type (α-MyHC) and the skeletal muscle type (β-MyHC), probably due to epitope spreading [50–52]. Altered expression of immunological self by MHC-II$^+$ APCs through expression of autoimmune-prone MHC (i.e., HLA-DQ8) and an excess amount of huAIRE/Aire (described in the present study) might be an interesting common feature for the development of muscle-specific autoimmunity.

The exact identity between huAIRE$^+$ peripheral APCs in our huAIRE-Tg and Aire$^+$ BM-derived non-conventional APCs in secondary lymphoid organs, eTACs [13,14], remains unknown. Although high MHC-II expression was observed in both huAIRE$^+$ peripheral APCs and eTACs, it has been reported that the latter population does not express the costimulatory molecule of CD86 [14]. More studies will be required to clarify the characteristics and function of Aire-expressing cells outside the thymus.

Finally, precise identification of Aire's target genes remains an important task for understanding the tolerance mechanisms that are established by Aire. Our transcriptomic analysis of mTECs overexpressing huAIRE/Aire from huAIRE-Tg, in combination with transcriptomic analysis of mTECs from Aire-deficient mice, might help us to characterize the target genes that are controlled by Aire *in vivo*.

Acknowledgements

We thank Drs. M. Yokoyama, D. Uchida, S. Shijie and N. Kuroda for establishing huAIRE-Tg. We thank Drs. D. Mathis and C. Benoist

for providing pDOI-5. We thank Ms. F. Hirota and R. Morita for technical assistance. We thank Dr. D.C. Chaplin for critical reading of the manuscript. We also thank Dr. Y. Kochi for helpful discussion. This work was supported in part by JSPS KAKENHI Grant Numbers JP16H06496 and JP16H05342, and AMED-CREST, Japan Agency for Medical Research and Development (M. Matsumoto).

Appendix A. Supplementary data

Supplementary data related to this article can be found at http://dx.doi.org/10.1016/j.jaut.2017.09.006.

References

[1] L. Klein, B. Kyewski, P.M. Allen, K.A. Hogquist, Positive and negative selection of the T cell repertoire: what thymocytes see (and don't see), Nat. Rev. Immunol. 14 (6) (2014) 377–391.
[2] J. Perera, L. Meng, F. Meng, H. Huang, Autoreactive thymic B cells are efficient antigen-presenting cells of cognate self-antigens for T cell negative selection, Proc. Natl. Acad. Sci. 110 (42) (2013) 17011–17016.
[3] T. Yamano, J. Nedjic, M. Hinterberger, M. Steinert, S. Koser, S. Pinto, N. Gerdes, E. Lutgens, N. Ishimaru, M. Busslinger, B. Brors, B. Kyewski, L. Klein, Thymic B cells are licensed to present self antigens for central T cell tolerance induction, Immunity 42 (6) (2015) 1048–1061.
[4] W. Yu, N. Jiang, P.J. Ebert, B.A. Kidd, S. Müller, P.J. Lund, J. Juang, K. Adachi, T. Tse, M.E. Birnbaum, E.W. Newell, D.M. Wilson, G.M. Grotenbreg, S. Valitutti, S.R. Quake, M.M. Davis, Clonal deletion prunes but does not eliminate self-specific αβ CD8(+) T lymphocytes, Immunity 42 (5) (2015) 929–941.
[5] F.P. Legoux, J.B. Lim, A.W. Cauley, S. Dikiy, J. Ertelt, T.J. Mariani, T. Sparwasser, S.S. Way, J.J. Moon, CD4+ T cell tolerance to tissue-restricted self antigens is mediated by antigen-specific regulatory T cells rather than deletion, Immunity 43 (5) (2015) 896–908.
[6] Y. Maeda, H. Nishikawa, D. Sugiyama, D. Ha, M. Hamaguchi, T. Saito, M. Nishioka, J.B. Wing, D. Adeegbe, I. Katayama, S. Sakaguchi, Detection of self-reactive CD8(+) T cells with an anergic phenotype in healthy individuals, Sci. (New York, N.Y.) 346 (6216) (2014) 1536–1540.
[7] D. Mathis, C. Benoist, Aire, Annu. Rev. Immunol. 27 (2009) 287–312.
[8] M.S. Anderson, E.S. Venanzi, Z. Chen, S.P. Berzins, C. Benoist, D. Mathis, The cellular mechanism of Aire control of T cell tolerance, Immunity 23 (2) (2005) 227–239.
[9] A. Liston, S. Lesage, J. Wilson, L. Peltonen, C.C. Goodnow, Aire regulates negative selection of organ-specific T cells, Nat. Immunol. 4 (4) (2003) 350–354.
[10] M.S. Anderson, E.S. Venanzi, L. Klein, Z. Chen, S.P. Berzins, S.J. Turley, H. von Boehmer, R. Bronson, A. Dierich, C. Benoist, D. Mathis, Projection of an immunological self shadow within the thymus by the aire protein, Sci. (New York, N.Y.) 298 (5597) (2002) 1395–1401.
[11] S. Yang, N. Fujikado, D. Kolodin, C. Benoist, D. Mathis, Immune tolerance. Regulatory T cells generated early in life play a distinct role in maintaining self-tolerance, Sci. (New York, N.Y.) 348 (6234) (2015) 589–594.
[12] S. Malchow, D.S. Leventhal, S. Nishi, B.I. Fischer, L. Shen, G.P. Paner, A.S. Amit, C. Kang, J.E. Geddes, J.P. Allison, N.D. Socci, P.A. Savage, Aire-dependent thymic development of tumor-associated regulatory T cells, Sci. (New York, N.Y.) 339 (6124) (2013) 1219–1224.
[13] J.M. Gardner, T.C. Metzger, E.J. McMahon, B.B. Au-Yeung, A.K. Krawisz, W. Lu, J.D. Price, K.P. Johannes, A.T. Satpathy, K.M. Murphy, K.V. Tarbell, A. Weiss, M.S. Anderson, Extrathymic Aire-expressing cells are a distinct bone marrow-derived population that induce functional inactivation of CD4(+) T cells, Immunity 39 (3) (2013) 560–572.
[14] J.M. Gardner, J.J. Devoss, R.S. Friedman, D.J. Wong, Y.X. Tan, X. Zhou, K.P. Johannes, M.A. Su, H.Y. Chang, M.F. Krummel, M.S. Anderson, Deletional tolerance mediated by extrathymic Aire-expressing cells, Sci. (New York, N.Y.) 321 (5890) (2008) 843–847.
[15] T.C. Metzger, M.S. Anderson, Control of central and peripheral tolerance by Aire, Immunol. Rev. 241 (1) (2011) 89–103.
[16] M. Nakayama, N. Abiru, H. Moriyama, N. Babaya, E. Liu, D. Miao, L. Yu, D.R. Wegmann, J.C. Hutton, J.F. Elliott, G.S. Eisenbarth, Prime role for an insulin epitope in the development of type 1 diabetes in NOD mice, Nature 435 (7039) (2005) 220–223.
[17] V. Kouskoff, H.J. Fehling, M. Lemeur, C. Benoist, D. Mathis, A vector driving the expression of foreign cDNAs in the MHC class II-positive cells of transgenic mice, J. Immunol. Methods 166 (2) (1993) 287–291.
[18] S. Niki, K. Oshikawa, Y. Mouri, F. Hirota, A. Matsushima, M. Yano, H. Han, Y. Bando, K. Izumi, M. Matsumoto, K.I. Nakayama, N. Kuroda, M. Matsumoto, Alteration of intra-pancreatic target-organ specificity by abrogation of Aire in NOD mice, J. Clin. Investig. 116 (5) (2006) 1292–1301.
[19] F.S. Wong, L. Wen, M. Tang, M. Ramanathan, I. Visintin, J. Daugherty, L.G. Hannum, C.A. Janeway Jr., M.J. Shlomchik, Investigation of the role of B-cells in type 1 diabetes in the NOD mouse, Diabetes 53 (10) (2004) 2581–2587.
[20] H. Noorchashm, Y.K. Lieu, N. Noorchashm, S.Y. Rostami, S.A. Greeley, A. Schlachterman, et al., I-Ag7-mediated antigen presentation by B lymphocytes is critical in overcoming a checkpoint in T cell tolerance to islet beta cells of nonobese diabetic mice, J. Immunol. 163 (1999) 743–750.
[21] M.J. Barnden, J. Allison, W.R. Heath, F.R. Carbone, Defective TCR expression in transgenic mice constructed using cDNA-based alpha- and beta-chain genes under the control of heterologous regulatory elements, Immunol. Cell Biol. 76 (1) (1998) 34–40.
[22] A.M. Gallegos, M.J. Bevan, Central tolerance to tissue-specific antigens mediated by direct and indirect antigen presentation, J. Exp. Med. 200 (8) (2004) 1039–1049.
[23] M. Yano, N. Kuroda, H. Han, M. Meguro-Horike, Y. Nishikawa, H. Kiyonari, K. Maemura, Y. Yanagawa, K. Obata, S. Takahashi, T. Ikawa, R. Satoh, H. Kawamoto, Y. Mouri, M. Matsumoto, Aire controls the differentiation program of thymic epithelial cells in the medulla for the establishment of self-tolerance, J. Exp. Med. 205 (12) (2008) 2827–2838.
[24] Y. Nishikawa, F. Hirota, M. Yano, H. Kitajima, J. Miyazaki, H. Kawamoto, Y. Mouri, M. Matsumoto, Biphasic Aire expression in early embryos and in medullary thymic epithelial cells before end-stage terminal differentiation, J. Exp. Med. 207 (5) (2010) 963–971.
[25] H. Nishijima, S. Kitano, H. Miyachi, J. Morimoto, H. Kawano, F. Hirota, R. Morita, Y. Mouri, K. Masuda, I. Imoto, K. Ikuta, M. Matsumoto, Ectopic aire expression in the thymic cortex reveals inherent properties of aire as a tolerogenic factor within the medulla, J. Immunol. Baltim. Md. 1950) 195 (10) (2015) 4641–4649.
[26] Y. Mouri, H. Nishijima, H. Kawano, F. Hirota, N. Sakaguchi, J. Morimoto, M. Matsumoto, NF-κB-inducing kinase in thymic stroma establishes central tolerance by orchestrating cross-talk with not only thymocytes but also dendritic cells, J. Immunol. Baltim. Md. 1950) 193 (9) (2014) 4356–4367.
[27] A.L. Caforio, M. Grazzini, J.M. Mann, P.J. Keeling, G.F. Bottazzo, W.J. McKenna, S. Schiaffino, Identification of alpha- and beta-cardiac myosin heavy chain isoforms as major autoantigens in dilated cardiomyopathy, Circulation 85 (5) (1992) 1734–1742.
[28] P. Venalis, I.E. Lundberg, Immune mechanisms in polymyositis and dermatomyositis and potential targets for therapy, Rheumatol. Oxf. Engl. 53 (3) (2014) 397–405.
[29] H. Lv, E. Havari, S. Pinto, R.V. Gottumukkala, L. Cornivelli, K. Raddassi, T. Matsui, A. Rosenzweig, R.T. Bronson, R. Smith, A.L. Fletcher, S.J. Turley, K. Wucherpfennig, B. Kyewski, M.A. Lipes, Impaired thymic tolerance to α-myosin directs autoimmunity to the heart in mice and humans, J. Clin. Investig. 121 (4) (2011) 1561–1573.
[30] A. Urasaki, G. Morvan, K. Kawakami, Functional dissection of the Tol2 transposable element identified the minimal cis-sequence and a highly repetitive sequence in the subterminal region essential for transposition, Genetics 174 (2) (2006) 639–649.
[31] F.X. Hubert, S.A. Kinkel, G.M. Davey, B. Phipson, S.N. Mueller, A. Liston, A.I. Proietto, P.Z. Cannon, S. Forehan, G.K. Smyth, L. Wu, C.C. Goodnow, F.R. Carbone, H.S. Scott, W.R. Heath, Aire regulates the transfer of antigen from mTECs to dendritic cells for induction of thymic tolerance, Blood 118 (9) (2011) 2462–2472.
[32] A. Chuprin, A. Avin, Y. Goldfarb, Y. Herzig, B. Levi, A. Jacob, A. Sela, S. Katz, M. Grossman, C. Guyon, M. Rathaus, H.Y. Cohen, I. Sagi, M. Giraud, M.W. McBurney, E.S. Husebye, J. Abramson, The deacetylase Sirt1 is an essential regulator of Aire-mediated induction of central immunological tolerance, Nat. Immunol. 16 (7) (2015) 737–745.
[33] M. Guerau-de-Arellano, D. Mathis, C. Benoist, Transcriptional impact of Aire varies with cell type, Proc. Natl. Acad. Sci. U. S. A. 105 (37) (2008) 14011–14016.
[34] M. Matsumoto, Y. Nishikawa, H. Nishijima, J. Morimoto, M. Matsumoto, Y. Mouri, Which model better fits the role of aire in the establishment of self-tolerance: the transcription model or the maturation model? Front. Immunol. 4 (2013) 210.
[35] X. Wang, M. Laan, R. Bichele, K. Kisand, H.S. Scott, P. Peterson, Post-Aire maturation of thymic medullary epithelial cells involves selective expression of keratinocyte-specific autoantigens, Front. Immunol. 3 (March) (2012) 19.
[36] N. Wada, K. Nishifuji, T. Yamada, J. Kudoh, N. Shimizu, M. Matsumoto, L. Peltonen, S. Nagafuchi, M. Amagai, Aire-dependent thymic expression of desmoglein 3, the autoantigen in pemphigus vulgaris, and its role in T-cell tolerance, J. Investig. Dermatol. 131 (2) (2011) 410–417.
[37] J. DeVoss, Y. Hou, K. Johannes, W. Lu, G.I. Liou, J. Rinn, H. Chang, R.R. Caspi, R. Caspi, L. Fong, M.S. Anderson, Spontaneous autoimmunity prevented by thymic expression of a single self-antigen, J. Exp. Med. 203 (12) (2006) 2727–2735.
[38] M. Giménez-Barcons, A. Casteràs, Mdel P. Armengol, E. Porta, P.A. Correa, A. Marín, R. Pujol-Borrell, R. Colobran, Autoimmune predisposition in Down syndrome may result from a partial central tolerance failure due to insufficient intrathymic expression of AIRE and peripheral antigens, J. Immunol. Baltim. Md. 1950) 193 (8) (2014) 3872–3879.
[39] Gabriel Skogberg, Vanja Lundberg, Susanne Lindgren, Judith Gudmundsdottir, Kerstin Sandström, Olle Kämpe, Göran Annerén, Jan Gustafsson, Jan Sunnegårdh, Sjoerd van der Post, Esbjörn Telemo, Martin Berglund, Olov Ekwall, Altered expression of autoimmune regulator in infant down syndrome thymus, a possible contributor to an autoimmune phenotype, J. Immunol. 193 (5) (2014) 2187–2195.
[40] F.A. Lima, C.A. Moreira-Filho, P.L. Ramos, H. Brentani, Lde A. Lima, M. Arrais,

L.C. Bento-de-Souza, L. Bento-de-Souza, M.I. Duarte, A. Coutinho, M. Carneiro-Sampaio, Decreased AIRE expression and global thymic hypofunction in Down syndrome, J. Immunol. Baltim. Md. 1950) 187 (6) (2011) 3422–3430.
[41] N. Tanahashi, H. Sato, S. Nogawa, T. Satoh, M. Kawamura, M. Shimoda, A case report of giant cell myocarditis and myositis observed during the clinical course of invasive thymoma associated with myasthenia gravis, Keio J. Med. 53 (2004) 30–42.
[42] J.W. Butany, P. McAuley, C. Bergeron, P. MacLaughlin, Giant cell myocarditis and myositis associated with thymoma and leprosy, Can. J. Cardiol. 7 (3) (1991) 141–145.
[43] A. Gidron, M. Quadrini, N. Dimov, A. Argiris, Malignant thymoma associated with fatal myocarditis and polymyositis in a 32-year-old woman with a history of hairy cell leukemia, Am. J. Clin. Oncol. 29 (2) (2006) 213–214.
[44] S. Levin, M. Schlesinger, Z. Handzel, T. Hahn, Y. Altman, B. Czernobilsky, J. Boss, Thymic deficiency in Down's syndrome, Pediatrics 63 (1) (1979) 80–87.
[45] L.M. Larocca, L. Lauriola, F.O. Ranelletti, M. Piantelli, N. Maggiano, R. Ricci, A. Capelli, Morphological and immunohistochemical study of Down syndrome thymus, Am. J. Med. Genet. Suppl. 7 (1990) 225–230.
[46] M.J. Bull, Committee on Genetics, Health supervision for children with Down syndrome, Pediatrics 128 (2) (2011) 393–406.
[47] C. Ramsey, O. Winqvist, L. Puhakka, M. Halonen, A. Moro, O. Kämpe, P. Eskelin, M. Pelto-Huikko, L. Peltonen, Aire deficient mice develop multiple features of APECED phenotype and show altered immune response, Hum. Mol. Genet. 11 (4) (2002) 397–409.
[48] N. Kuroda, T. Mitani, N. Takeda, N. Ishimaru, R. Arakaki, Y. Hayashi, Y. Bando, K. Izumi, T. Takahashi, T. Nomura, S. Sakaguchi, T. Ueno, Y. Takahama, D. Uchida, S. Sun, F. Kajiura, Y. Mouri, H. Han, A. Matsushima, G. Yamada, M. Matsumoto, Development of autoimmunity against transcriptionally unrepressed target antigen in the thymus of aire-deficient mice, J. Immunol. 174 (4) (2005) 1862–1870.
[49] F.X. Hubert, S.A. Kinkel, P.E. Crewther, P.Z. Cannon, K.E. Webster, M. Link, R. Uibo, M.K. O'Bryan, A. Meager, S.P. Forehan, G.K. Smyth, L. Mittaz, S.E. Antonarakis, P. Peterson, W.R. Heath, H.S. Scott, Aire-deficient C57BL/6 mice mimicking the common human 13-base pair deletion mutation present with only a mild autoimmune phenotype, J. Immunol. Baltim. Md. 1950) 182 (6) (2009) 3902–3918.
[50] S.L. Hayward, N. Bautista-Lopez, K. Suzuki, A. Atrazhev, P. Dickie, J.F. Elliott, CD4 T cells play major effector role and CD8 T cells initiating role in spontaneous autoimmune myocarditis of HLA-DQ8 transgenic IAb knockout non-obese diabetic mice, J. Immunol. Baltim. Md. 1950) 176 (12) (2006) 7715–7725.
[51] J.F. Elliott, J. Liu, Z.N. Yuan, N. Bautista-Lopez, S.L. Wallbank, K. Suzuki, D. Rayner, P. Nation, M.A. Robertson, G. Liu, K.M. Kavanagh, Autoimmune cardiomyopathy and heart block develop spontaneously in HLA-DQ8 transgenic IAbeta knockout NOD mice, Proc. Natl. Acad. Sci. U. S. A. 100 (23) (2003) 13447–13452.
[52] J.A. Taylor, E. Havari, M.F. McInerney, R. Bronson, K.W. Wucherpfennig, M.A. Lipes, A spontaneous model for autoimmune myocarditis using the human MHC molecule HLA-DQ8, J. Immunol. Baltim. Md. 1950) 172 (4) (2004) 2651–2658.